

# Zinc amidinate-catalysed cyclization reaction of carbodiimide and alkynes. An insight into the mechanism.

Blanca Parra-Cadenas<sup>a</sup>, Carlos Ginés<sup>a</sup>, Daniel García-Vivó<sup>b</sup>, David Elorriaga<sup>b\*</sup> and Fernando Carrillo-Hermosilla<sup>a\*</sup>

<sup>a</sup> Departamento de Química Inorgánica, Orgánica y Bioquímica-Centro de Innovación en Química Avanzada (ORFEO-CINQA), Facultad de Ciencias y Tecnologías Químicas, Universidad de Castilla-La Mancha, 13071 Ciudad Real, Spain

[fernando.carrillo@uclm.es]

<sup>b</sup> Departamento de Química Orgánica e Inorgánica, Instituto Universitario de Química Organometálica “Enrique Moles”, Universidad de Oviedo, Julián Clavería 8, 33006 Oviedo, Spain.

[elorriagadavid@uniovi.es]

## 1.- General Methods and Materials

All manipulations were performed under a nitrogen atmosphere using standard Schlenk and glove-box techniques. The solvents used for the syntheses and for the NMR experiments were all anhydrous. All reagents were obtained from commercial suppliers (Sigma Aldrich) and used without further purification, with the exception of *N,N'*-bis(2,6-dimethylphenyl)carbodiimide, which was synthesized as described previously.<sup>1</sup> Commercial ZnEt<sub>2</sub> solutions in toluene were always handled inside the glovebox.

NMR spectra were recorded on BRUKER INOVA 400 and 500 MHz spectrometers. <sup>13</sup>C and <sup>19</sup>F spectra were proton decoupled. <sup>1</sup>H and <sup>13</sup>C NMR spectra were referenced against the appropriate solvent signal. Characterisation details, including <sup>1</sup>H, <sup>13</sup>C{<sup>1</sup>H} and <sup>19</sup>F{<sup>1</sup>H} (when necessary) NMR spectra, for compounds **4a-g**, **4a-D<sub>2</sub>**, **5** and **6** are included in the following sections of this Supporting Information. HRMS were measured in ESI mode, with a TOF mass analyser (Bruker model Impact II).

## 2.- Experimental procedure and characterisation details

### 2.1.- General procedure for the synthesis of 2,4-dihydropyridines, compounds **4a-g**.

Syntheses of compounds **4a-g** were performed under N<sub>2</sub> atmosphere. In the glovebox, in a vial, *m* equivalents of the appropriate alkyne (**3a-g**, *X* mol) were dissolved in 0.5 mL of C<sub>6</sub>D<sub>6</sub>, followed by the addition of 10 mol% of ZnEt<sub>2</sub> (15% mol solution in Toluene, 3·10<sup>-5</sup> mol). Subsequently, 1 equivalent of the appropriate

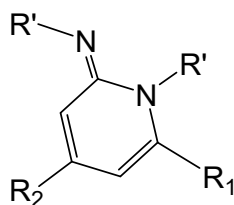
carbodiimide (**2a-b**,  $3 \cdot 10^{-4}$  mol) was added. The reaction mixture was then added to a Young NMR tube and heated at 120°C for 4 days (6 hours for **4g**).

<i>2,4-dihydropyridine</i>	<i>Number of equivalents of alkyne needed (m)</i>	<i>Number of mol of alkyne needed (X)</i>
<b>4a</b>	2	$6 \cdot 10^{-4}$
<b>4b</b>	2	$6 \cdot 10^{-4}$
<b>4c</b>	3	$9 \cdot 10^{-4}$
<b>4d</b>	2	$6 \cdot 10^{-4}$
<b>4e</b>	2	$6 \cdot 10^{-4}$
<b>4f</b>	2	$6 \cdot 10^{-4}$
<b>4g</b>	6	$1,8 \cdot 10^{-3}$

*Table 1. Number of equivalents (m) and mol (X) of alkyne needed for the synthesis of 2,4-dihydropyridines 4a-g.*

Syntheses of compound **4e** was performed under N<sub>2</sub> atmosphere. In the glovebox, in a vial, 1 equivalent of propiolamidine **5a** ( $3 \cdot 10^{-4}$  mol) was dissolved in 0.5 mL of C<sub>6</sub>D<sub>6</sub>, followed by the addition of 10 mol% of ZnEt<sub>2</sub> (15% mol solution in Toluene,  $3 \cdot 10^{-5}$  mol). Subsequently, 1 equivalent of phenylacetylene **3b** ( $3 \cdot 10^{-4}$  mol) was added. The reaction mixture was then added to a Young NMR tube and heated at 120°C for 4 days.

Separation and purification of compounds **4a-e** and **4g** were carried out by adding pentane to the previous solution, where **yellowish** crystals of the desired 2,4-dihydropyridines were obtained as. Separation and purification of compound **4f** was carried out by using a silica gel column chromatography (hexane/ethyl acetate = 4:1) **obtaining a yellow solid**.



**(4)**

<i>2,4-dihydropyridine</i>	$R_1$	$R_2$	$R'$	Yield (mg/ %)	
<b>4a</b>	Ph	Ph	2,6-diisopropylphenyl	143	82
<b>4b</b>	p-CH <sub>3</sub> O-Ph	p-CH <sub>3</sub> O-Ph	2,6-diisopropylphenyl	150	80
<b>4c</b>	p-F-Ph	p-F-Ph	2,6-diisopropylphenyl	137	76
<b>4d</b>	p-N(CH <sub>3</sub> ) <sub>2</sub> -Ph	p-N(CH <sub>3</sub> ) <sub>2</sub> -Ph	2,6-diisopropylphenyl	153	78
<b>4e</b>	p-CH <sub>3</sub> O-Ph	Ph	2,6-diisopropylphenyl	152	85
<b>4a-D<sub>2</sub></b>	Ph-CCD	Ph-CCD	2,6-diisopropylphenyl	141	83
<b>4f</b>	Ph	Ph	2,6-dimethylphenyl	14	10
<b>4g</b>	CH <sub>3</sub> OO-CCH	CH <sub>3</sub> OO-CCH	2,6-diisopropylphenyl	133	84

**Table 2.** Substituents ( $R_1$ ,  $R_2$  and  $R'$ ) and *isolated* yields of 2,4-dihydropyridines **4a-g**, **4a-D<sub>2</sub>**.

## 2.2.- General procedure for the synthesis of propiolamidine **5a**.

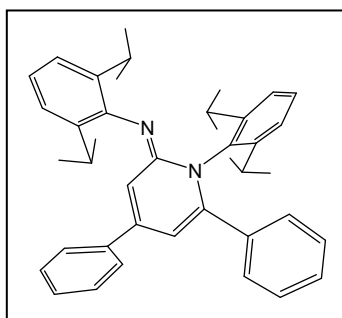
For the preparation of compound **5a** we extended our previous methodology which used ZnEt<sub>2</sub> as precatalyst.<sup>2</sup> The synthesis was performed under N<sub>2</sub> atmosphere. In a Schlenk equipped with a Young valve, 1 equivalent of alkyne **3a** (2·10<sup>-3</sup> mol) was dissolved in 5 mL of toluene, followed by the addition of 3 mol% of ZnEt<sub>2</sub> **1** (15% mol solution in Toluene, 6·10<sup>-5</sup> mol). Subsequently, 1 equivalent of N,N'-bis(2,6-diisopropylphenyl)carbodiimide **2a** (2·10<sup>-3</sup> mol) was added and the solution was stirred for 4h at 120°C. The solvent was eliminated in vacuo. Then, 5 mL of pentane were added and stirred for 3h. After eliminating the solvent under reduced pressure compound **5** was obtained as a beige powder with good yield (82%).

## 2.3.- General procedure for the synthesis of zinc bisamidinate, compound **6**.

Thus, in a Young Schlenk and under N<sub>2</sub> atmosphere 2 equivalents of propiolamidine **5a** (1·10<sup>-3</sup> mol) were dissolved in 3 mL of toluene. Subsequently, 1 equivalent ZnEt<sub>2</sub>

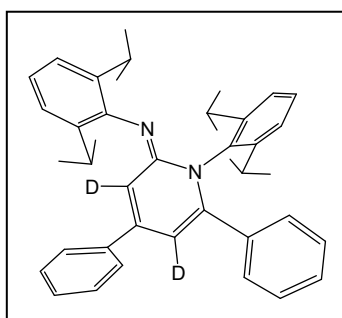
(15% mol solution in Toluene) ( $1 \cdot 10^{-3}$  mol) was added. The solution was stirred for 16 h at room temperature. The solvent was removed under reduced pressure and 5 mL of hexane were then added and placed at  $-20$  °C for 24 hours. After filtration and drying under reduced pressure, compound **6** was obtained as a beige powder with excellent yield (93%).

#### 2.4.- Characterisation details



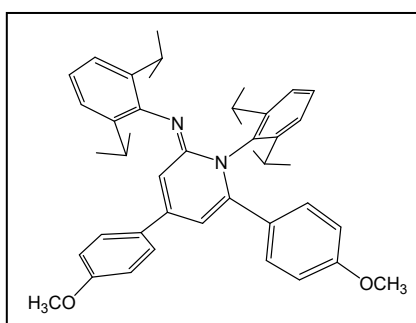
**4a:**  $^1\text{H}$  NMR ( $\text{C}_6\text{D}_6$ )  $\delta$  (ppm) = 0.94 (d,  $J$  = 6.8 Hz, 6H,  $\text{CH}_3$ ), 1.13 (d,  $J$  = 6.8 Hz, 6H,  $\text{CH}_3$ ), 1.32 (d,  $J$  = 6.9 Hz, 6H,  $\text{CH}_3$ ), 1.38 (d,  $J$  = 6.8 Hz, 6H,  $\text{CH}_3$ ), 3.33-3.36 (m, 2H, CH), 3.38-3.42 (m, 2H, CH), 6.26 (d,  $J$  = 2 Hz, 1H, =CH), 6.75 (d,  $J$  = 2 Hz, 1H, =CH), 6.83-6.87 (m, 3Harom), 6.93-6.96 (m, 3Harom), 6.98-7.00 (m, 1Harom), 7.11-7.18 (m, 4Harom), 7.23-7.27 (m, 3Harom), 7.35-7.37 (m, 2Harom).

$^{13}\text{C}\{^1\text{H}\}$  NMR ( $\text{C}_6\text{D}_6$ )  $\delta$  (ppm) = 23.9 (2C), 24.6 (2C), 24.9 (2C), 25.2 (2C), 28.1 (2C), 29.5 (2), 105.8, 111.4, 123.2, 124.0, 124.6, 126.4, 127.8, 128.4, 128.7, 129.1, 129.4, 130.1, 136.4, 137.1, 137.8, 140.4, 145.6, 145.9, 146.7, 150.0, 154.4. **HRMS:  $m/z$  567.37 ( $\text{M} + \text{H}^+$ ).**



**4a-D<sub>2</sub>:**  $^1\text{H}$  NMR ( $\text{C}_6\text{D}_6$ )  $\delta$  (ppm) = 0.94 (d,  $J$  = 6.8 Hz, 6H,  $\text{CH}_3$ ), 1.13 (d,  $J$  = 6.8 Hz, 6H,  $\text{CH}_3$ ), 1.32 (d,  $J$  = 6.8 Hz, 6H,  $\text{CH}_3$ ), 1.38 (d,  $J$  = 6.8 Hz, 6H,  $\text{CH}_3$ ), 3.32-3.43 (m, 4H, CH), 6.83-6.88 (m, 3Harom), 6.93-7.01 (m, 5Harom), 7.11-7.18 (m, 3Harom), 7.22-7.27 (m, 3Harom), 7.35-7.37 (m, 2Harom).  $^{13}\text{C}\{^1\text{H}\}$  NMR ( $\text{C}_6\text{D}_6$ )  $\delta$  (ppm) = 23.5, 24.2, 24.5, 24.9, 27.7, 29.1, 122.8, 123.7, 124.2, 126.1, 127.4,

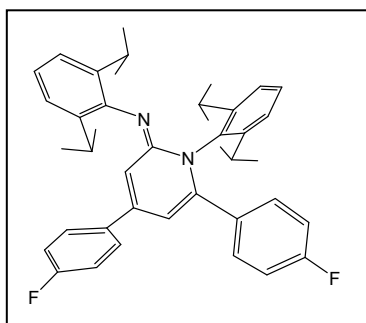
127.6, 127.8, 128.0, 128.3, 128.7, 129.1, 129.8, 136.1, 136.7, 137.4, 140.0, 145.1, 145.6, 146.4, 150.1, 154.1. **HRMS:  $m/z$  569.37 ( $\text{M} + \text{H}^+$ ).**



**4b:**  $^1\text{H}$  NMR ( $\text{C}_6\text{D}_6$ )  $\delta$  (ppm) = 1.01 (d,  $J$  = 6.4 Hz, 6H,  $\text{CH}_3$ ), 1.17 (d,  $J$  = 6.6 Hz, 6H,  $\text{CH}_3$ ), 1.37 (d,  $J$  = 6.6 Hz, 6H,  $\text{CH}_3$ ), 1.42 (d,  $J$  = 6.5 Hz, 6H,  $\text{CH}_3$ ), 3.21 (s, 3H,  $\text{OCH}_3$ ), 3.09 (s, 3H,  $\text{OCH}_3$ ), 3.39-3.50 (m, 4H, CH), 6.36 (d,  $J$  = 2 Hz, 1H, =CH), 6.51-6.55 (m,

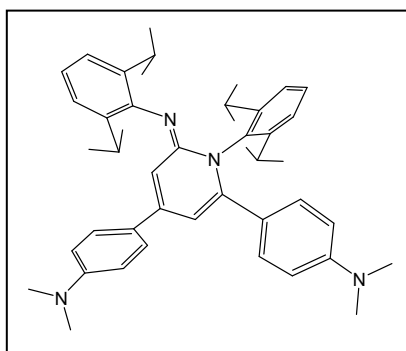
4Harom), 6.73 (d,  $J = 2$  Hz, 1H, =CH), 6.93-6.95 (m, 3Harom), 7.19-7.37 (m, 7Harom).  $^{13}\text{C}\{^1\text{H}\}$  NMR ( $\text{C}_6\text{D}_6$ )  $\delta$  (ppm) = 24.0 (2C), 24.6 (2C), 25.0 (2C), 25.2 (2C), 28.0 (2C), 29.5 (2C), 54.7, 54.8, 105.2, 109.7, 113.2, 114.6, 123.0, 124.0, 124.6, 128.6, 128.9, 129.4, 130.0, 131.6, 137.4, 140.5, 145.1, 146.3, 146.8, 150.2, 154.7, 160.3, 160.8.

**HRMS:  $m/z$  627.39 ( $\text{M} + \text{H}^+$ ).**



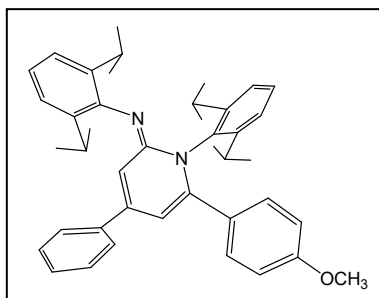
**4c:**  $^1\text{H}$  NMR ( $\text{C}_6\text{D}_6$ )  $\delta$  (ppm) = 0.90 (d,  $J = 6.8$  Hz, 6H,  $\text{CH}_3$ ), 1.13 (d,  $J = 6.8$  Hz, 6H,  $\text{CH}_3$ ), 1.31 (d,  $J = 6.9$  Hz, 6H,  $\text{CH}_3$ ), 1.36 (d,  $J = 6.8$  Hz, 6H,  $\text{CH}_3$ ), 3.23-3.28 (m, 2H, CH), 3.33-3.38 (m, 4H, CH), 5.99 (d,  $J = 2$  Hz, 1H, =CH), 6.49-6.52 (m, 2Harom), 6.57-6.60 (m, 2Harom), 6.61 (d,  $J = 2$  Hz, 1H, =CH), 6.73-6.76 (m, 2Harom), 7.08-7.12 (m, 4Harom), 7.20-7.26 (m, 4Harom).  $^{13}\text{C}\{^1\text{H}\}$

NMR ( $\text{C}_6\text{D}_6$ )  $\delta$  (ppm) = 23.8 (2C), 24.5 (2C), 24.9 (2C), 25.2 (2C), 28.1 (2C), 29.4 (2C), 105.4, 111.3, 114.7, 114.9, 116.0, 116.1, 123.4, 124.1, 124.7, 127.6, 128.6, 129.6, 132.0, 133.7, 136.8, 140.3, 144.4, 145.7, 146.6, 149.5, 154.1.  $^{19}\text{F}$  NMR ( $\text{C}_6\text{D}_6$ )  $\delta$  (ppm) = -112.2, -112.1. **HRMS:  $m/z$  603.39 ( $\text{M} + \text{H}^+$ ).**

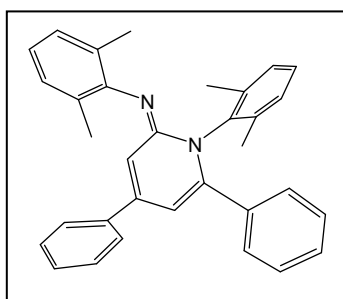


**4d:**  $^1\text{H}$  NMR ( $\text{C}_6\text{D}_6$ )  $\delta$  (ppm) = 1.10 (d,  $J = 6.8$  Hz, 6H,  $\text{CH}_3$ ), 1.19 (d,  $J = 7.3$  Hz, 6H,  $\text{CH}_3$ ), 1.40 (d,  $J = 6.9$  Hz, 6H,  $\text{CH}_3$ ), 1.44 (d,  $J = 6.9$  Hz, 6H,  $\text{CH}_3$ ), 2.29 (s, 6H,  $\text{CH}_3$ ), 2.41 (s, 6H,  $\text{CH}_3$ ), 3.50-3.57 (m, 4H, CH), 6.26-6.31 (m, 4Harom), 6.63 (d,  $J = 2$  Hz, 1H, =CH), 6.77 (d,  $J = 2$  Hz, 1H, =CH), 7.03-7.05 (m, 2Harom), 7.19-7.23 (m, 3Harom), 7.31-7.34 (m,

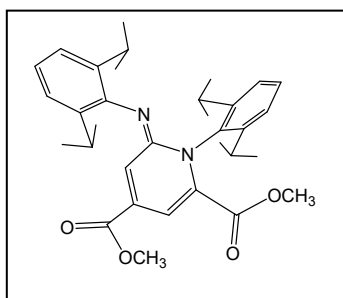
3Harom), 7.52-7.53 (m, 2Harom).  $^{13}\text{C}\{^1\text{H}\}$  NMR ( $\text{C}_6\text{D}_6$ )  $\delta$  (ppm) = 24.2 (2C), 24.6 (2C), 25.1 (2C), 25.2 (2C), 28.0 (2C), 29.6(2C), 39.5 (2C), 39.8 (2C), 104.5, 107.7, 111.1, 112.6, 122.7, 123.9, 124.5, 125.4, 127.4, 127.9, 129.1, 131.3, 138.0, 140.8, 145.5, 147.0, 147.1, 150.4, 150.7, 151.1, 155.2. **HRMS:  $m/z$  653.46 ( $\text{M} + \text{H}^+$ ).**



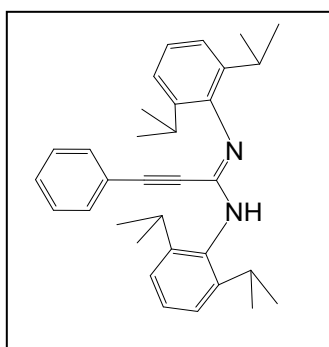
**4e:**  $^1\text{H}$  NMR ( $\text{C}_6\text{D}_6$ )  $\delta$  (ppm) = 1.01 (d,  $J$  = 6.8 Hz, 6H,  $\text{CH}_3$ ), 1.14 (d,  $J$  = 6.8 Hz, 6H,  $\text{CH}_3$ ), 1.33 (d,  $J$  = 6.9 Hz, 6H,  $\text{CH}_3$ ), 1.40 (d,  $J$  = 6.8 Hz, 6H,  $\text{CH}_3$ ), 3.09 (s, 3H,  $\text{OCH}_3$ ), 3.35-3.46 (m, 4H, CH), 6.31 (d,  $J$  = 2 Hz, 1H, =CH), 6.50-6.52 (m, 2Harom), 6.74 (d,  $J$  = 2 Hz, 1H, =CH), 6.91-7.01 (m, 6Harom), 7.15-7.19 (m, 2Harom), 7.25-7.29 (m, 3Harom), 7.39-7.42 (m, 2Harom).  $^{13}\text{C}\{^1\text{H}\}$  NMR ( $\text{C}_6\text{D}_6$ )  $\delta$  (ppm) = 24.0 (2C), 24.6 (2C), 24.9 (2C), 25.2 (2C), 28.1 (2C), 29.5 (2C), 54.7, 105.3, 110.9, 113.3, 123.1, 124.0, 124.6, 126.5, 128.8, 129.0, 129.1, 129.4, 131.6, 137.4, 138.1, 140.4, 145.8, 146.1, 146.8, 150.4, 154.6, 160.3. **HRMS:  $m/z$  597.38 ( $\text{M} + \text{H}^+$ ).**



**4f:**  $^1\text{H}$  NMR ( $\text{C}_6\text{D}_6$ )  $\delta$  (ppm) = 2.27 (s, 3H,  $\text{CH}_3$ ), 2.30 (s, 3H,  $\text{CH}_3$ ), 6.09 (d,  $J$  = 2 Hz, 1H, =CH), 6.61 (d,  $J$  = 2 Hz, 1H, =CH), 6.81-7.03 (m, 11Harom), 7.15-7.15 (m, 3Harom), 7.30-7.32 (m, 2Harom).  $^{13}\text{C}\{^1\text{H}\}$  NMR ( $\text{C}_6\text{D}_6$ )  $\delta$  (ppm) = 18.9 (2C), 19.2 (2C), 104.9, 109.9, 121.9, 126.7, 127.8, 127.9, 128.2, 128.3, 128.4, 128.5, 128.7, 129.0, 129.3, 136.4, 136.5, 138.3, 139.8, 146.9, 149.1, 150.1, 151.4. **HRMS:  $m/z$  455.24 ( $\text{M} + \text{H}^+$ ).**

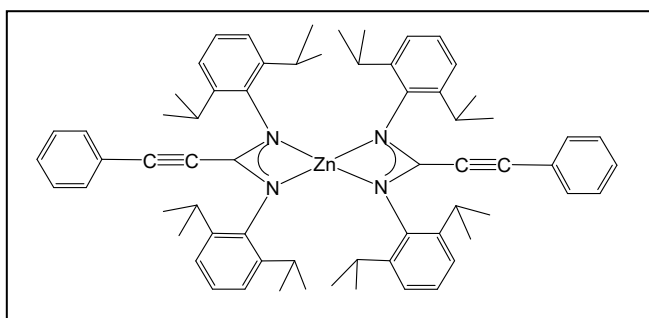


**4g:**  $^1\text{H}$  NMR ( $\text{C}_6\text{D}_6$ )  $\delta$  (ppm) = 1.15 (d,  $J$  = 6.8 Hz, 6H,  $\text{CH}_3$ ), 1.19 (d,  $J$  = 6.8 Hz, 6H,  $\text{CH}_3$ ), 1.35 (d,  $J$  = 6.8 Hz, 6H,  $\text{CH}_3$ ), 1.39 (d,  $J$  = 6.9 Hz, 6H,  $\text{CH}_3$ ), 2.57 (s, 3H,  $\text{OCH}_3$ ), 3.17-3.29 (m, 4H, CH), 3.36 (s, 3H,  $\text{OCH}_3$ ), 5.18 (d,  $J$  = 14 Hz, 1H, =CH), 7.04-7.22 (m, 6Harom), 9.75 (d,  $J$  = 14 Hz, 1H, =CH).  $^{13}\text{C}\{^1\text{H}\}$  NMR ( $\text{C}_6\text{D}_6$ )  $\delta$  (ppm) = 23.5, 24.0, 24.3, 25.0, 29.0, 29.1, 50.9, 52.1, 73.6, 88.1, 101.9, 123.7, 125.2, 127.4, 127.9, 128.2, 128.7, 131.0, 133.1, 138.4, 147.6, 151.7, 167.3. **HRMS:  $m/z$  531.31 ( $\text{M} + \text{H}^+$ ).**



**5a:**  $^1\text{H}$  NMR ( $\text{C}_6\text{D}_6$ )  $\delta$  (ppm) = 1.16 (bs, 11H,  $\text{CH}_3$ ), 1.40 (d,  $J$  = 7.1 Hz, 13H,  $\text{CH}_3$ ), 3.69 (m, 4H, CH), 6.65-6.73 (m, 5Harom), 7.19-7.25 (m, 6Harom), 11.80 (bs, 1H, NH).  $^{13}\text{C}\{^1\text{H}\}$  NMR ( $\text{C}_6\text{D}_6$ )  $\delta$  (ppm) = 23.3 (4C), 24.8 (4C), 28.8

(4C), 80.7, 97.1, 121.0, 123.4 (2C), 126.1, 128.4 (2C), 129.6, 132.4 (2C), 140.5, 144.7 (2C), 149.1.



**6:**  $^1\text{H}$  NMR ( $\text{C}_6\text{D}_6$ )  $\delta$  (ppm) = 1.14 (bs, 24H,  $\text{CH}_3$ ), 1.38 (d,  $J = 6.9$  Hz, 24H,  $\text{CH}_3$ ), 3.66-3.69 (m, 8H, CH), 6.55-6.71 (m, 10Harom), 7.15 (m, 12Harom).  $^{13}\text{C}\{^1\text{H}\}$  NMR ( $\text{C}_6\text{D}_6$ )  $\delta$  (ppm) = 23.1 (8C), 24.5 (8C), 29.2 (8C), 80.0 (2C), 99.3

(2C), 120.8 (2C), 123.1 (4C), 125.6 (2C), 128.4 (4C), 129.8 (2C), 132.6 (4C), 141.5 (2C), 144.7 (4C), 160.3 (2C).

### 3.- NMR spectra

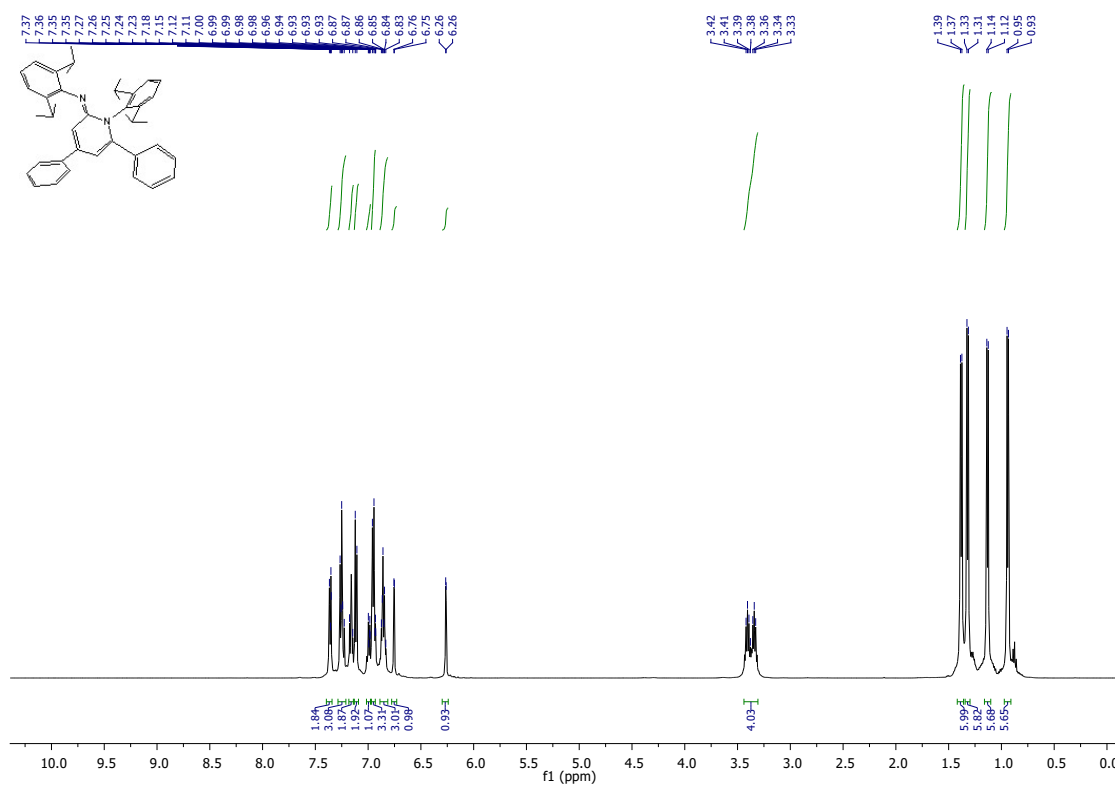


Figure S1.  $^1\text{H}$ -NMR full chart for **4a** in  $\text{C}_6\text{D}_6$ .

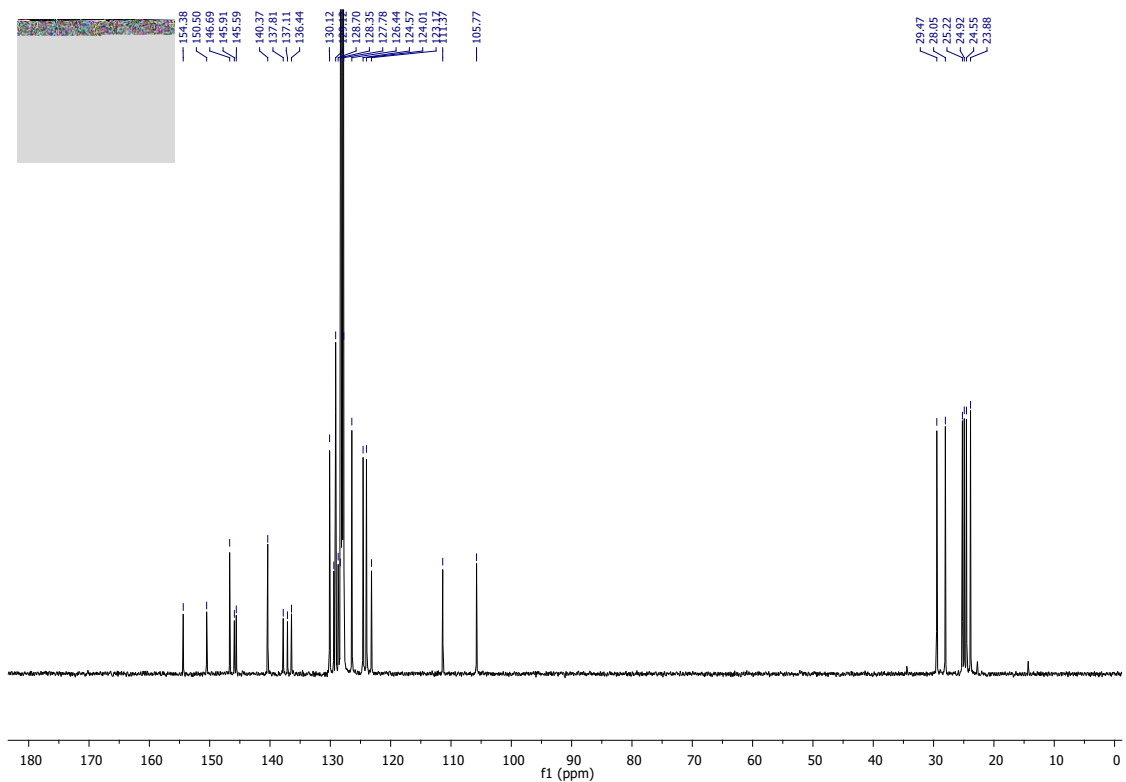


Figure S2.  $^{13}\text{C}$ -NMR full chart for **4a** in  $\text{C}_6\text{D}_6$ .

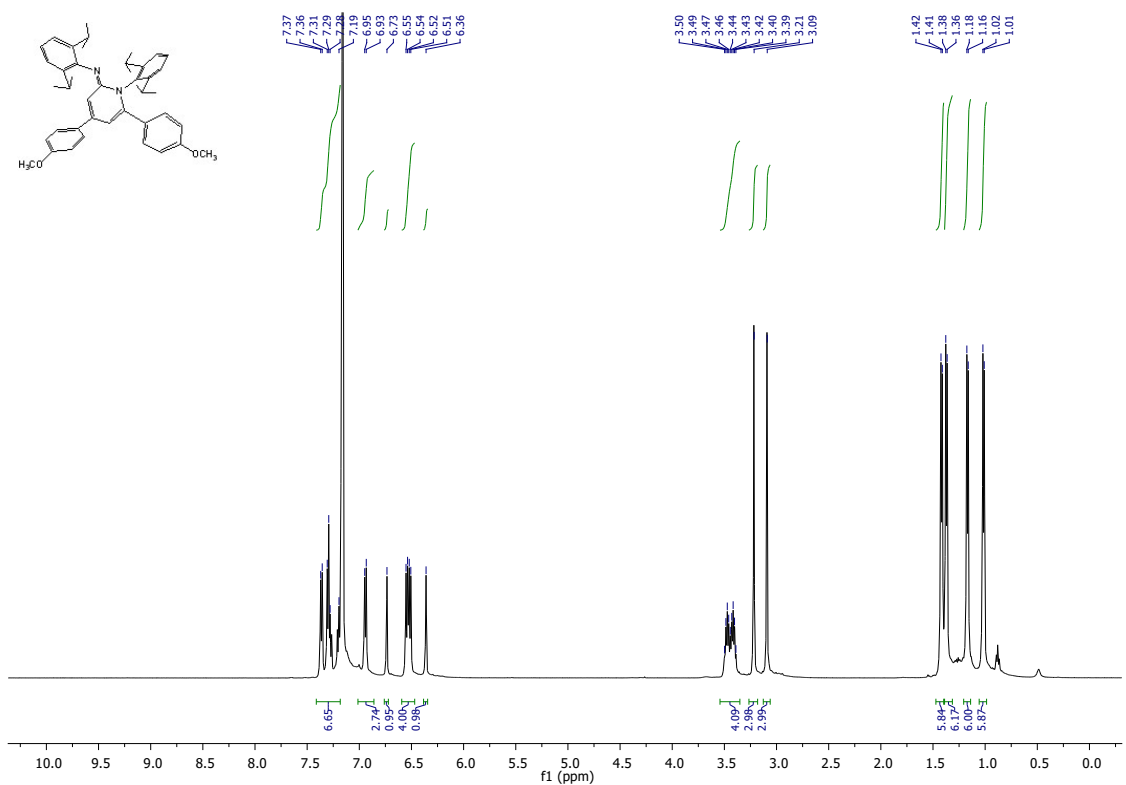


Figure S3.  $^1\text{H}$ -NMR full chart for **4b** in  $\text{C}_6\text{D}_6$ .

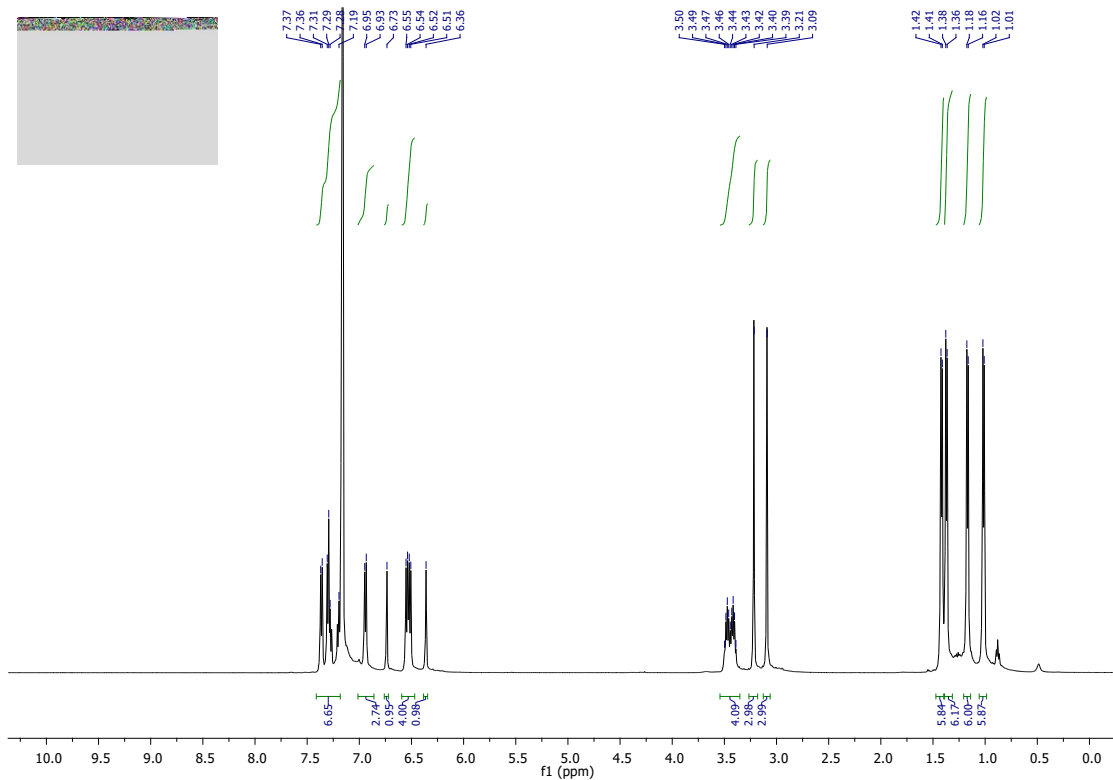


Figure S4.  $^{13}\text{C}$ -NMR full chart for **4b** in  $\text{C}_6\text{D}_6$ .

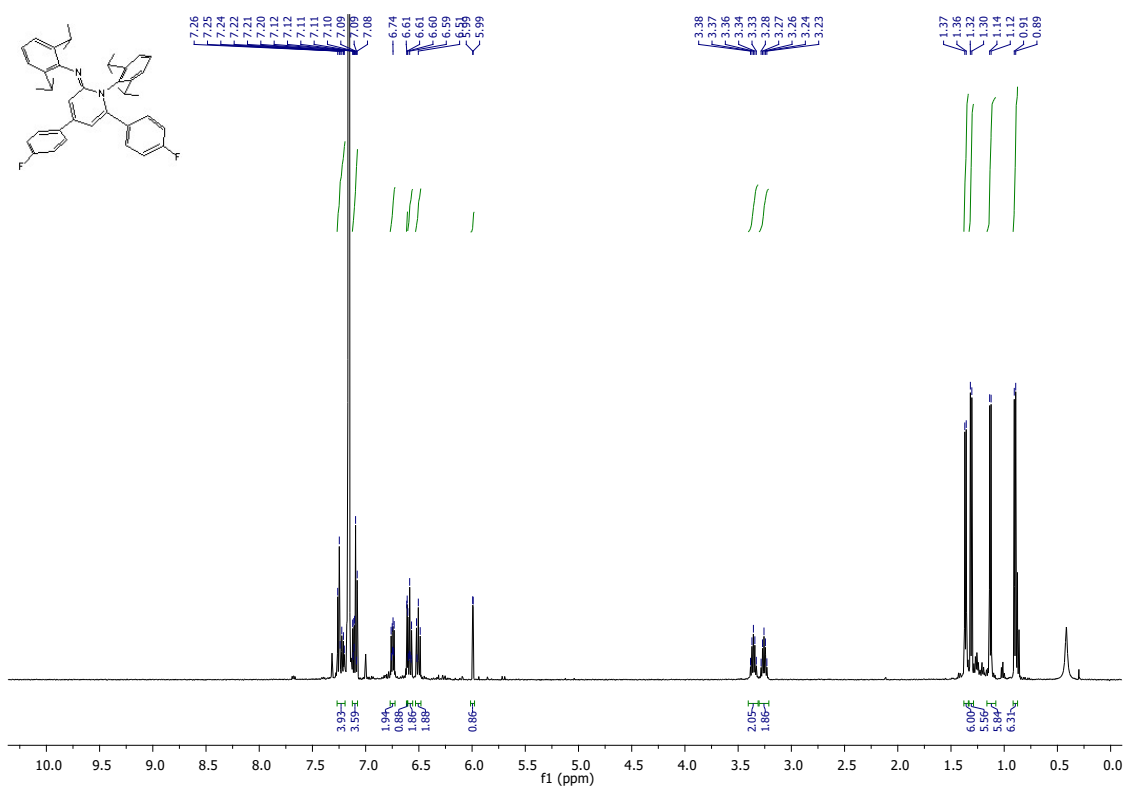


Figure S5.  $^1\text{H}$ -NMR full chart for **4c** in  $\text{C}_6\text{D}_6$ .

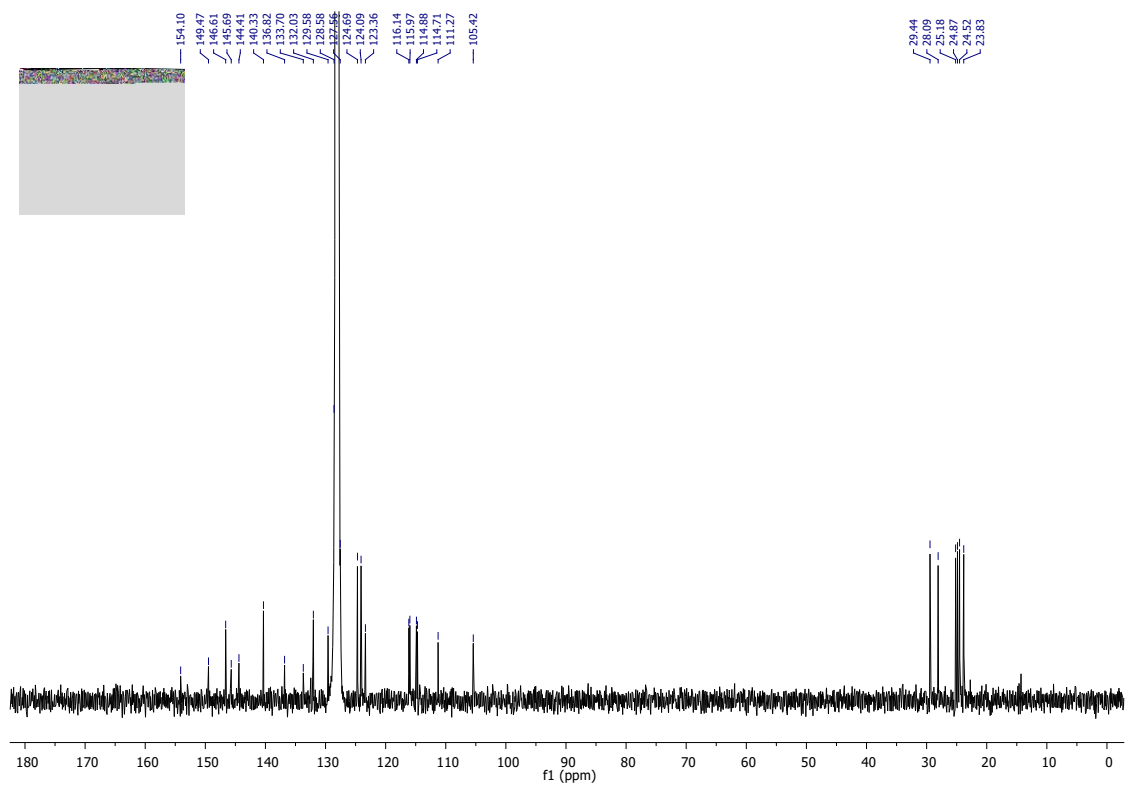


Figure S6.  $^{13}\text{C}$ -NMR full chart for **4c** in  $\text{C}_6\text{D}_6$ .

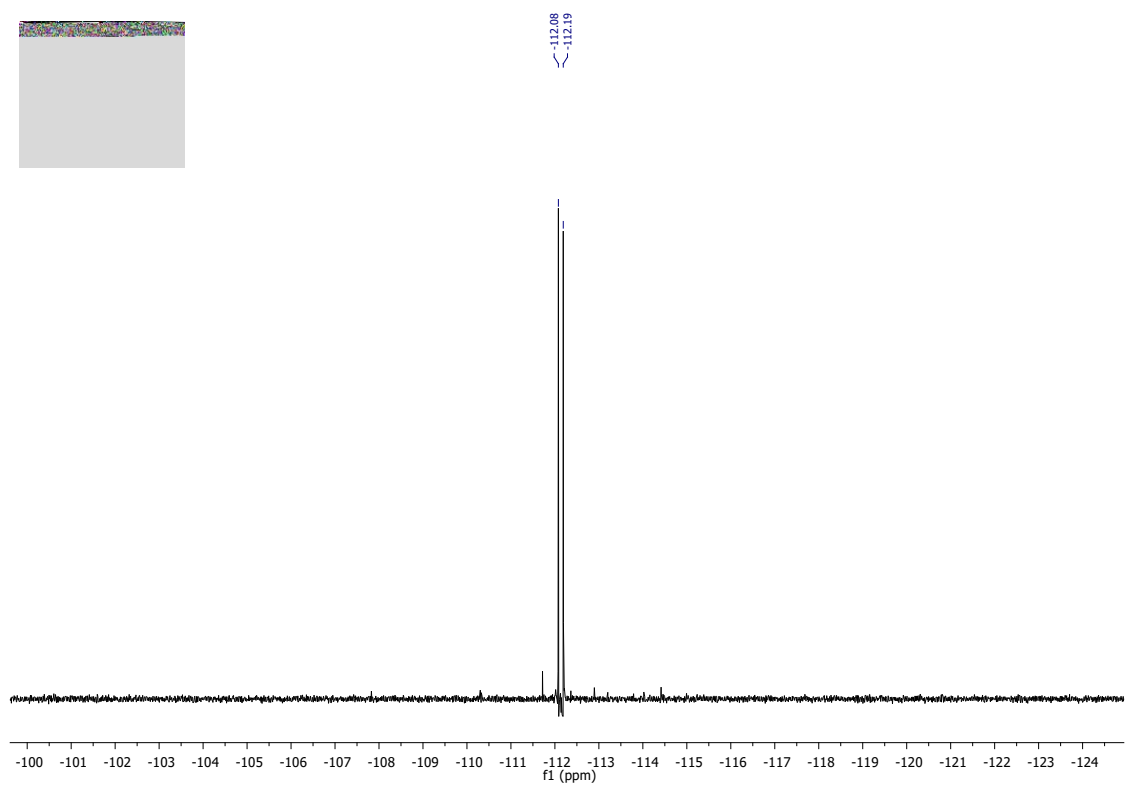


Figure S7.  $^{19}\text{F}$ -NMR full chart for **4c** in  $\text{C}_6\text{D}_6$ .

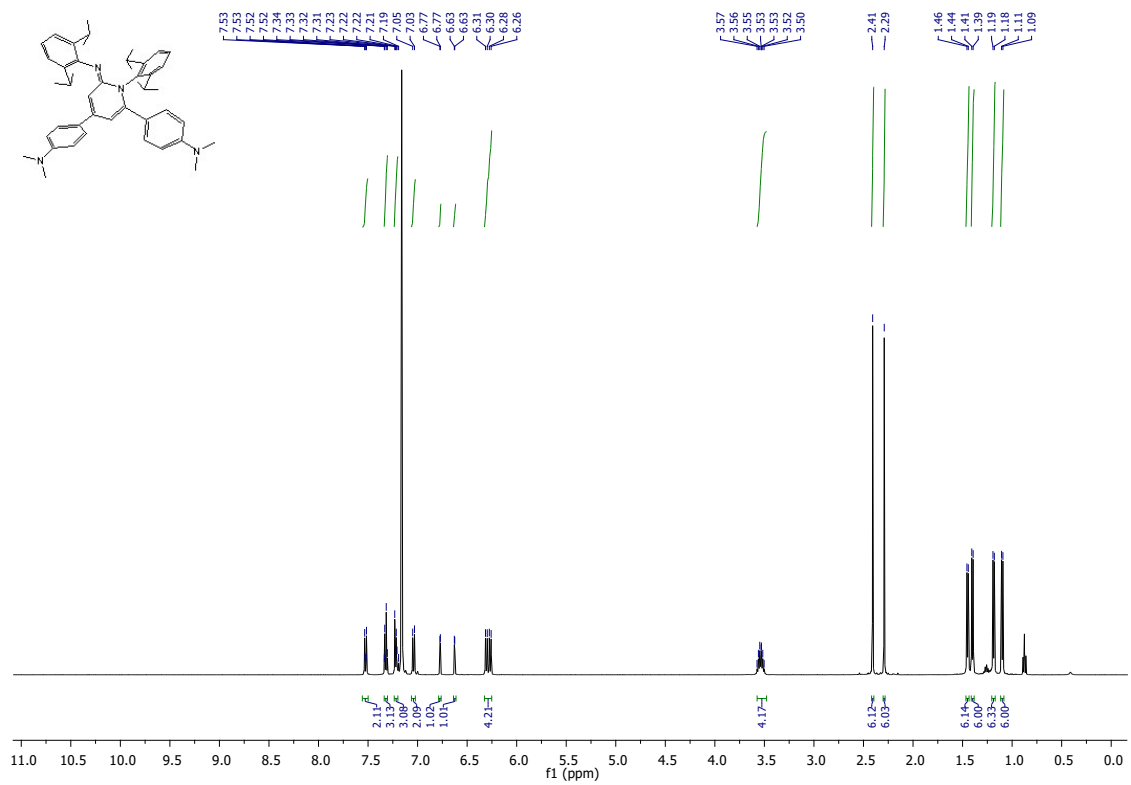


Figure S8.  $^1\text{H-NMR}$  full chart for **4d** in  $\text{C}_6\text{D}_6$ .

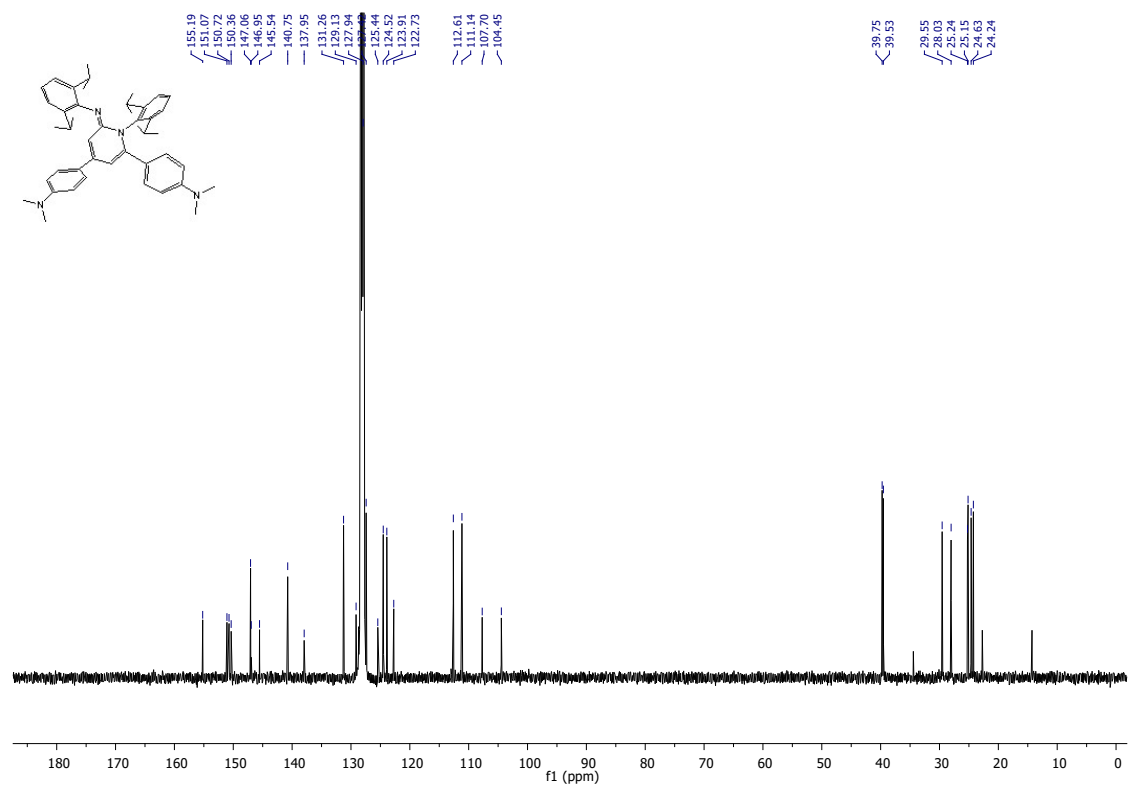
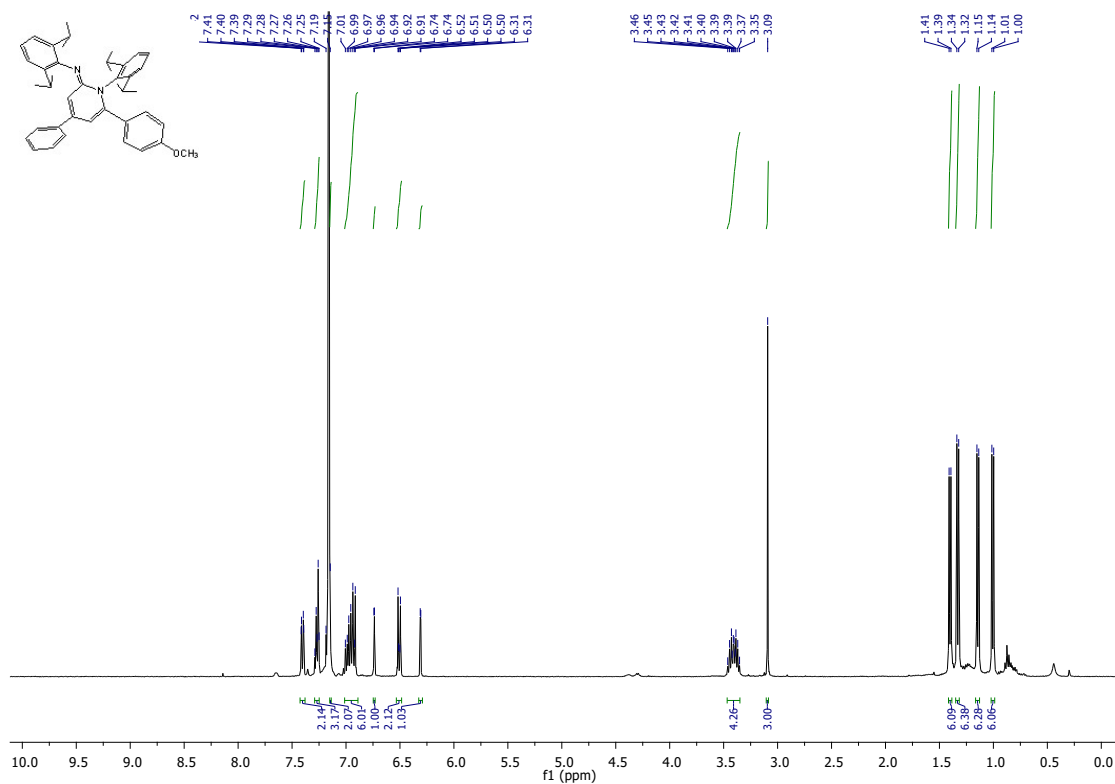
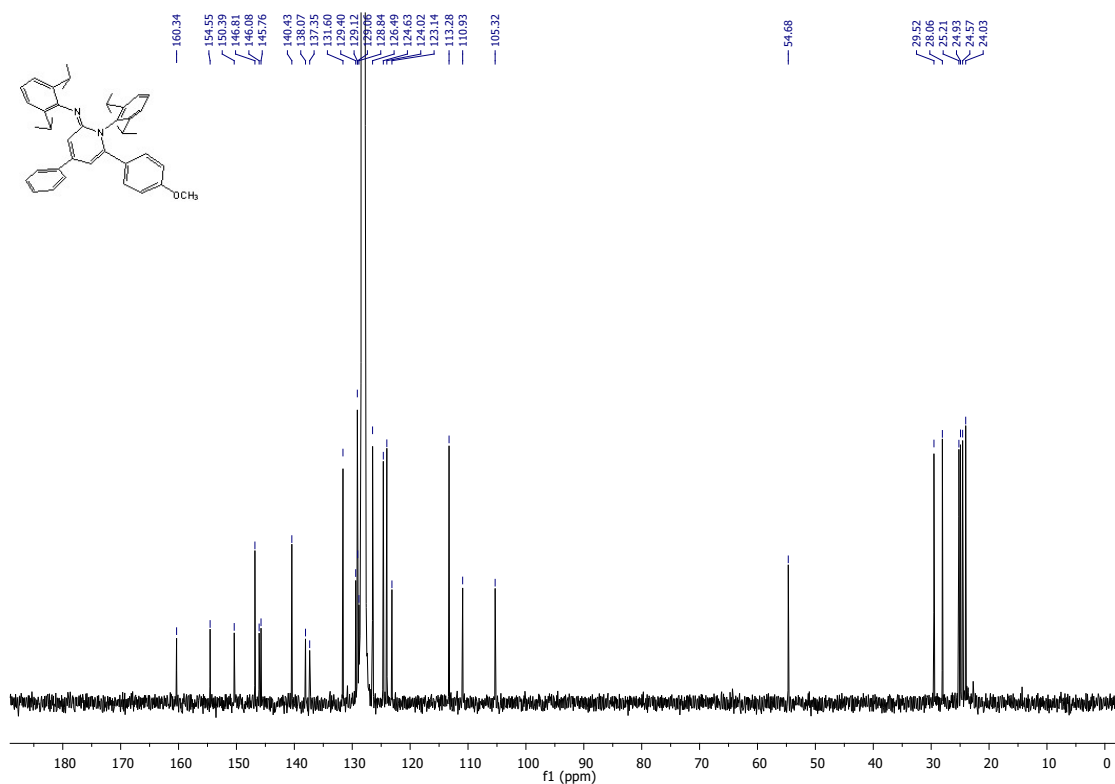


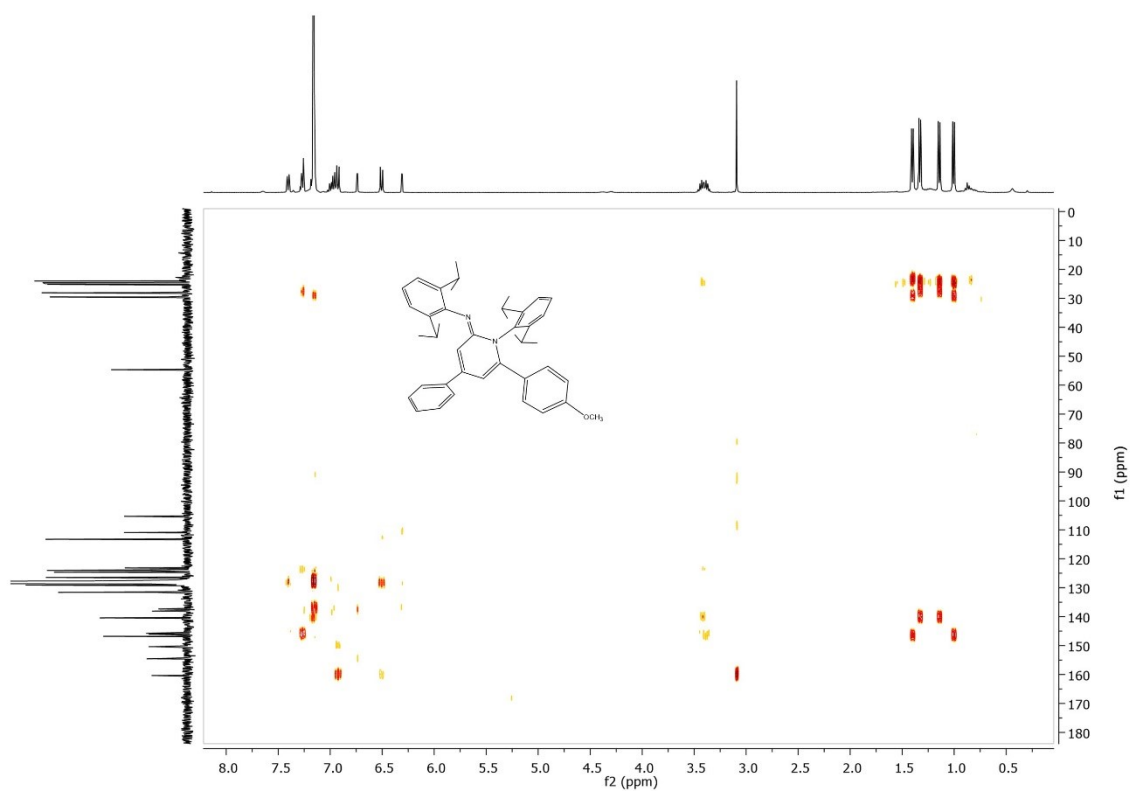
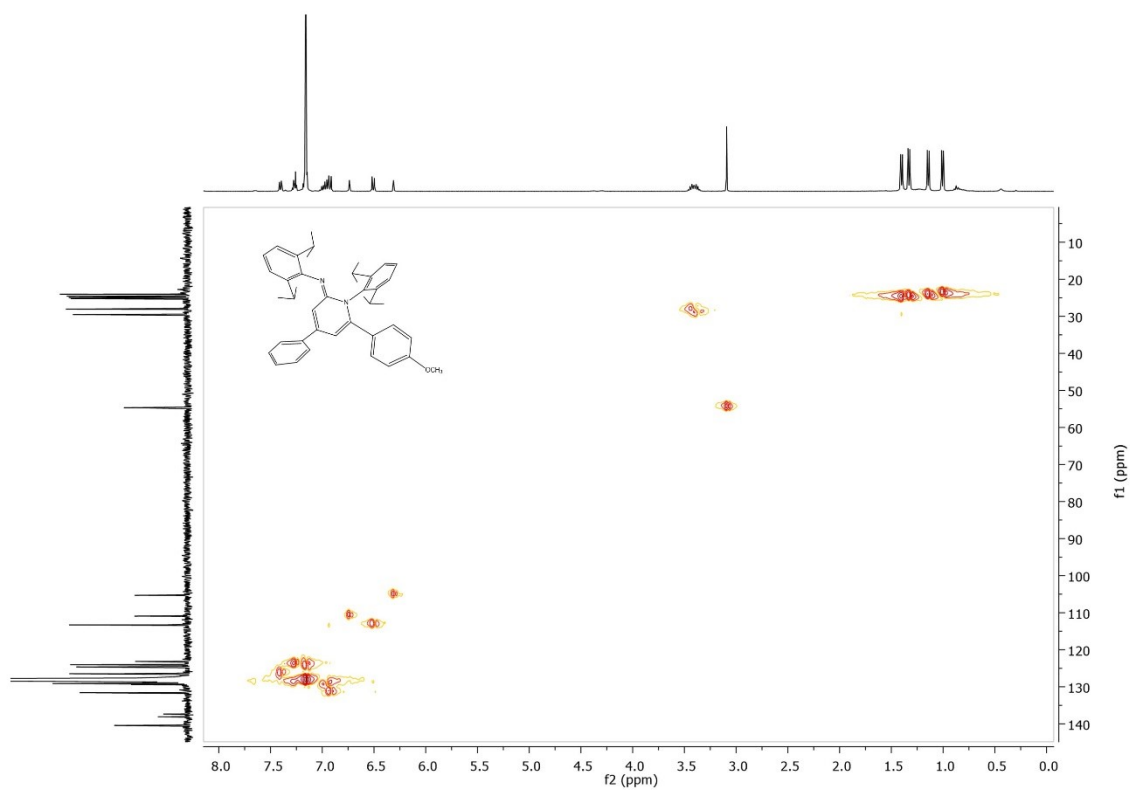
Figure S9.  $^{13}\text{C-NMR}$  full chart for **4d** in  $\text{C}_6\text{D}_6$ .



**Figure S10.** <sup>1</sup>H-NMR full chart for **4e** in C<sub>6</sub>D<sub>6</sub>.



**Figure S11.** <sup>13</sup>C-NMR full chart for **4e** in C<sub>6</sub>D<sub>6</sub>.



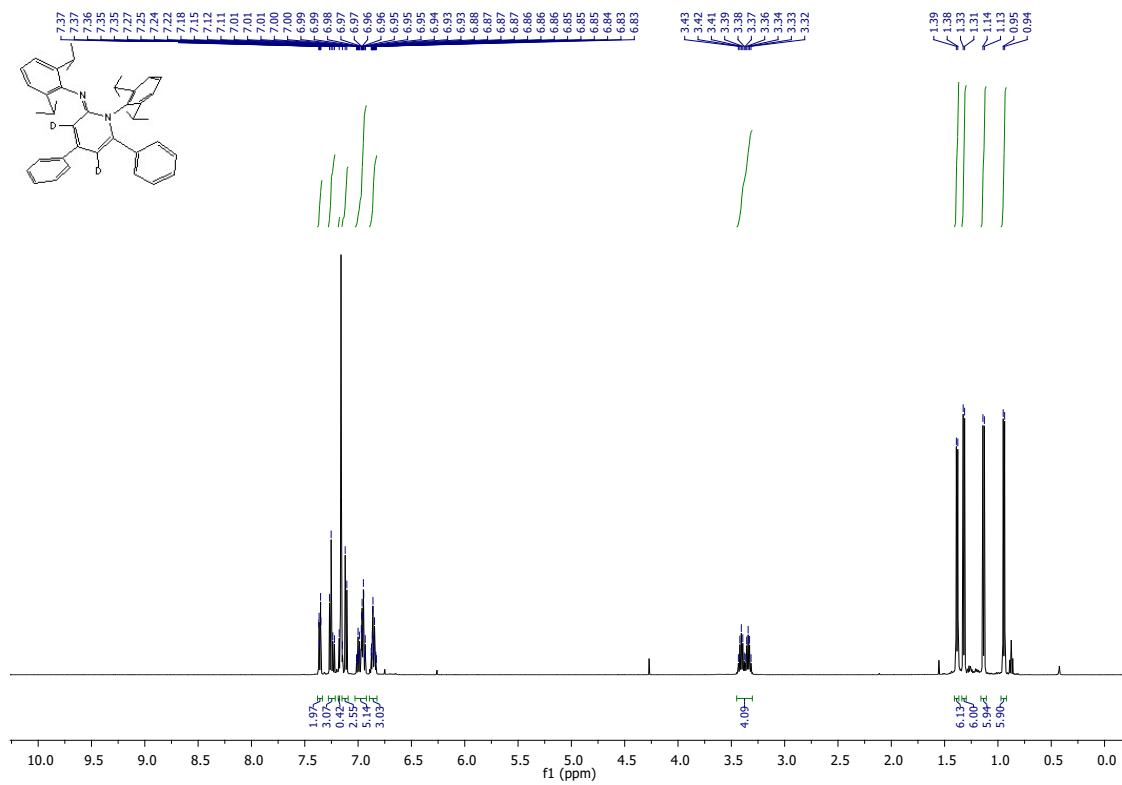


Figure S14. <sup>1</sup>H-NMR full chart for 4a-D<sub>2</sub> in C<sub>6</sub>D<sub>6</sub>.

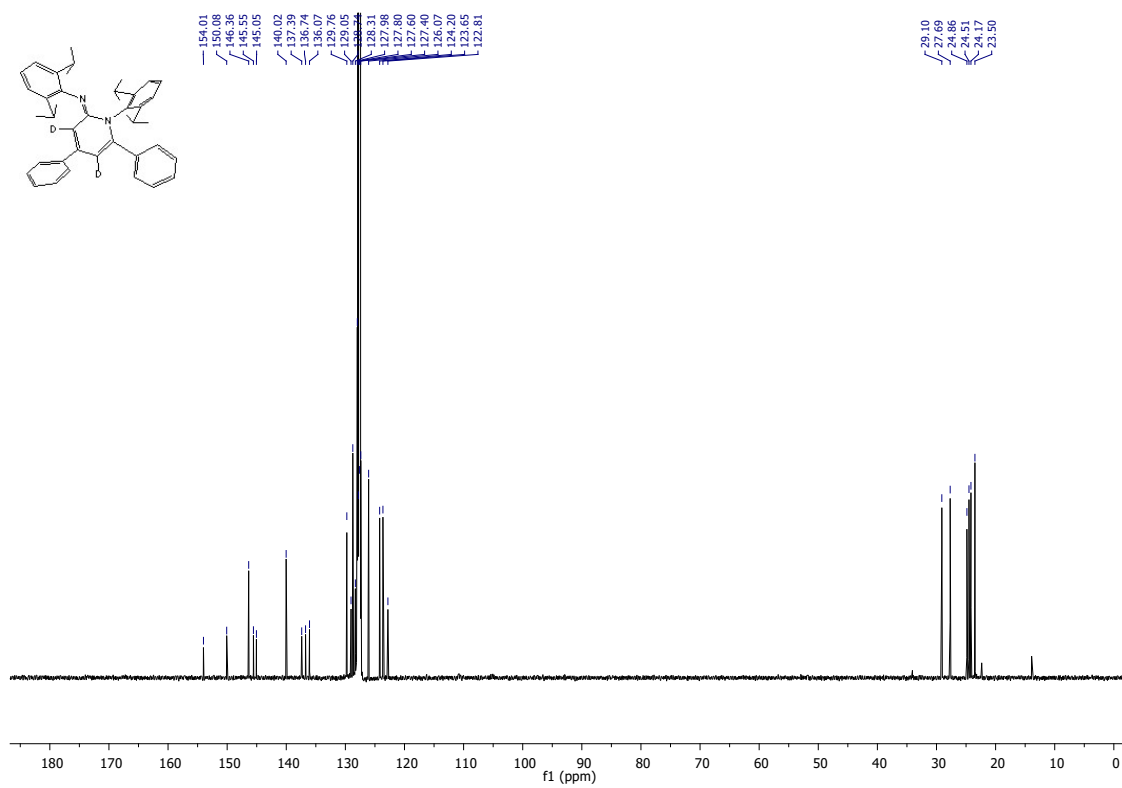


Figure S15. <sup>13</sup>C-NMR full chart for 4a-D<sub>2</sub> in C<sub>6</sub>D<sub>6</sub>.

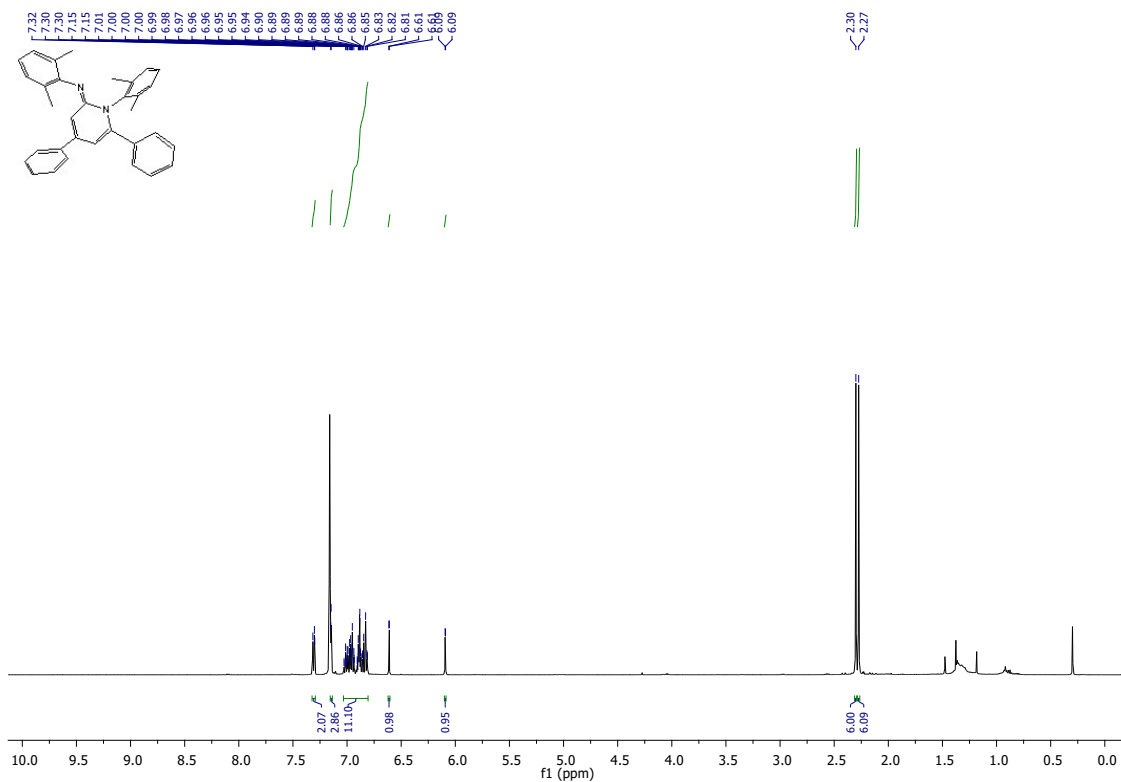


Figure S16. <sup>1</sup>H-NMR full chart for **4f** in C<sub>6</sub>D<sub>6</sub>.

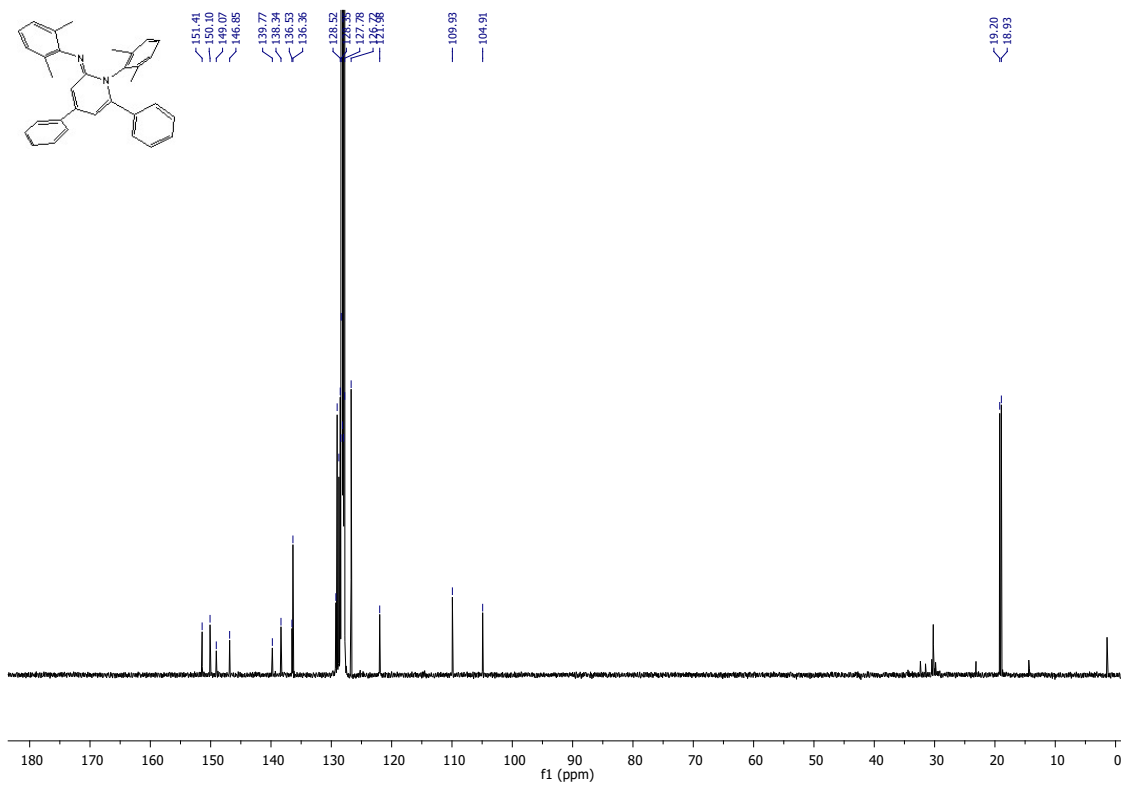
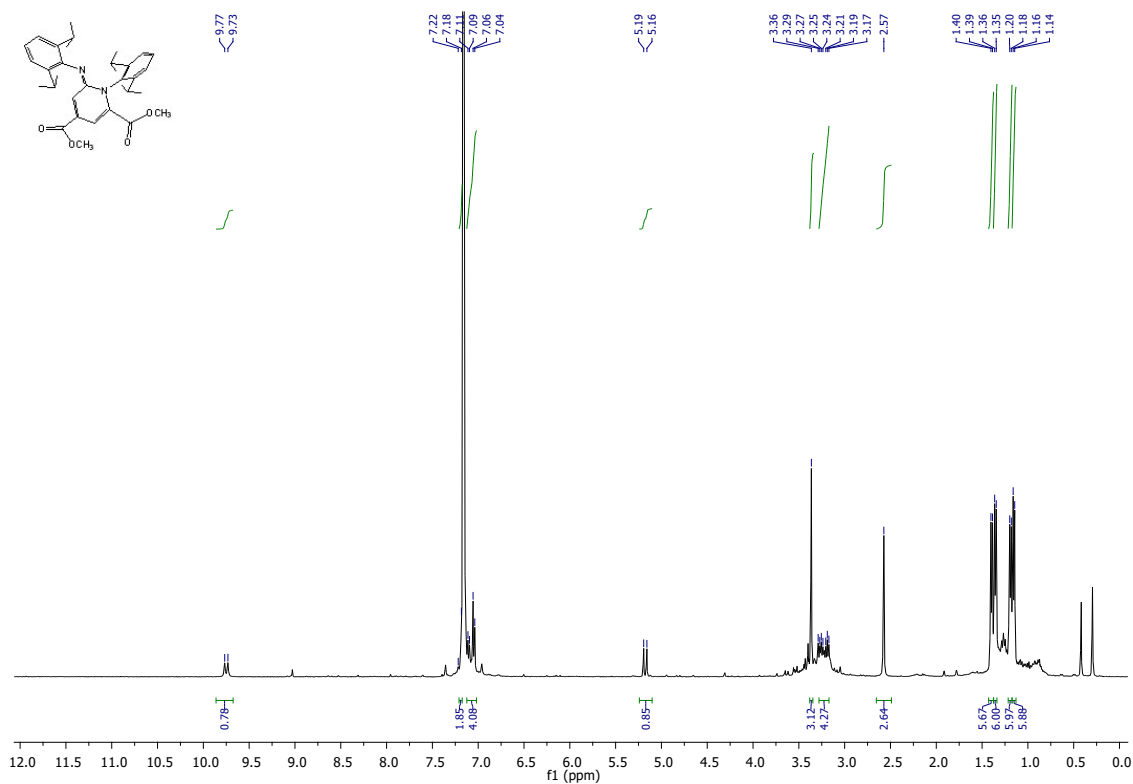
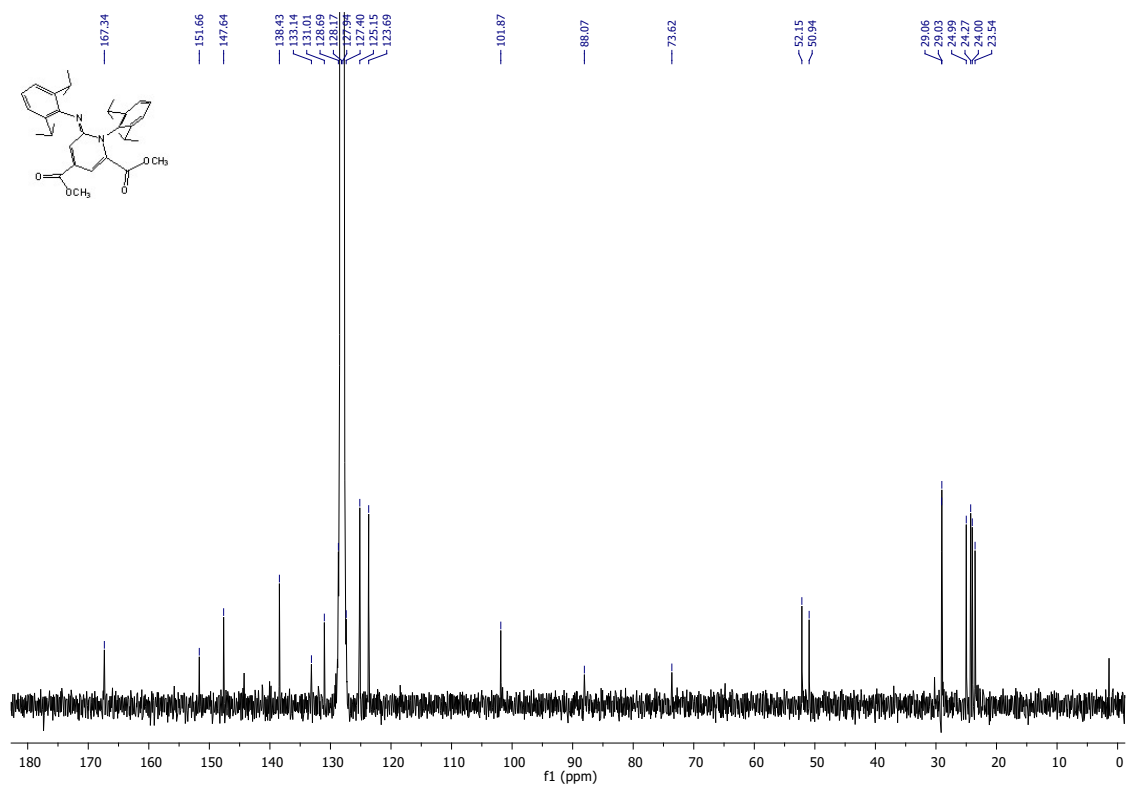


Figure S17. <sup>13</sup>C-NMR full chart for **4f** in C<sub>6</sub>D<sub>6</sub>.



**Figure S18. <sup>1</sup>H-NMR full chart for 4g in C<sub>6</sub>D<sub>6</sub>.**



**Figure S19. <sup>13</sup>C-NMR full chart for 4g in C<sub>6</sub>D<sub>6</sub>.**

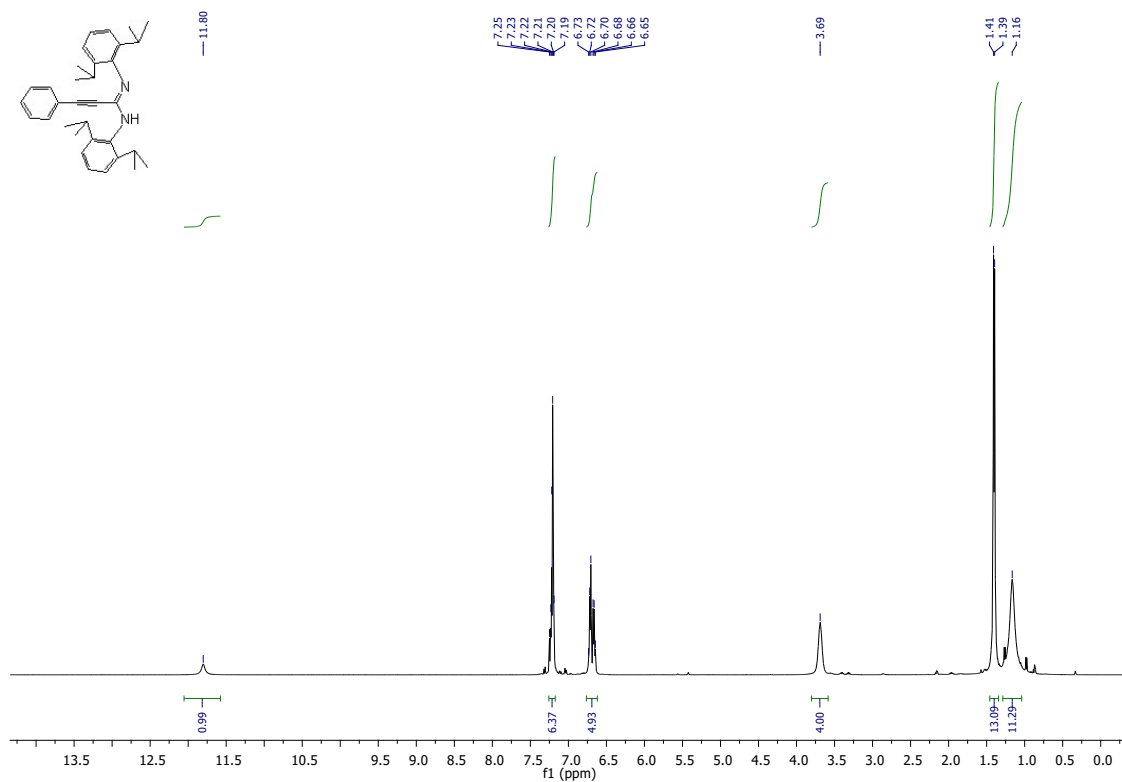


**Figure S20.**  $^1\text{H-NMR}$  full chart for **5a** in  $\text{C}_6\text{D}_6$ .

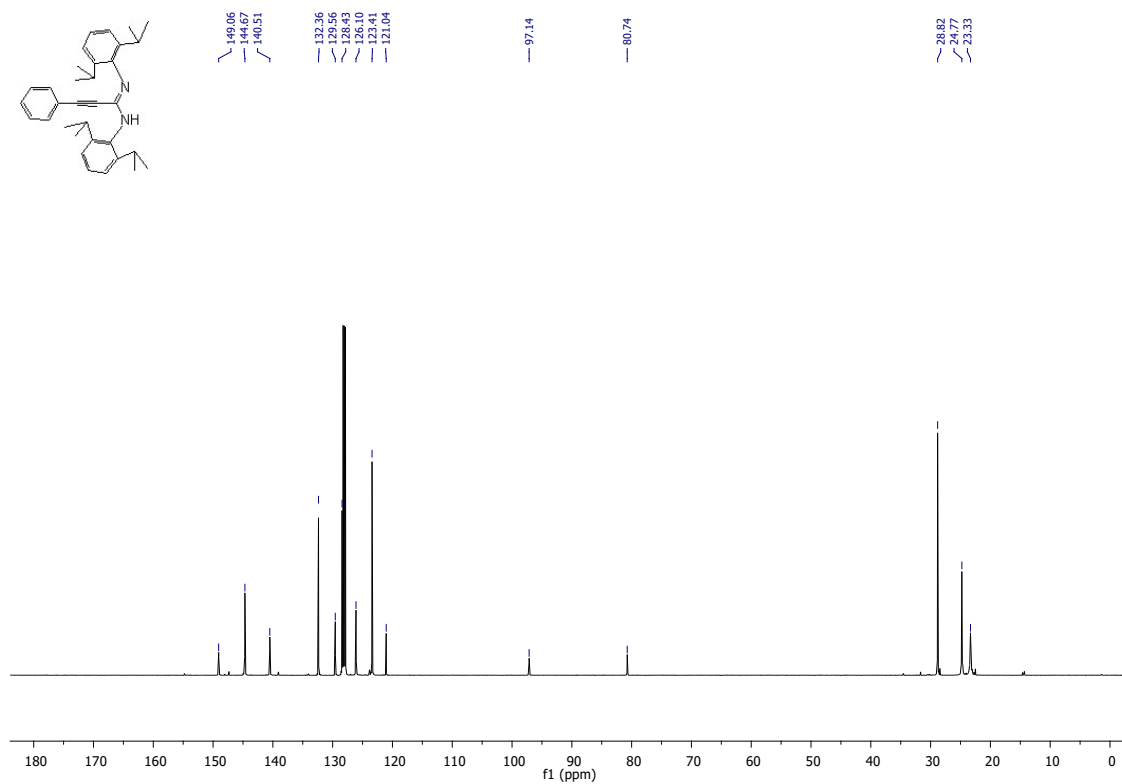


**Figure S21.**  $^{13}\text{C-NMR}$  full chart for **5a** in  $\text{C}_6\text{D}_6$ .

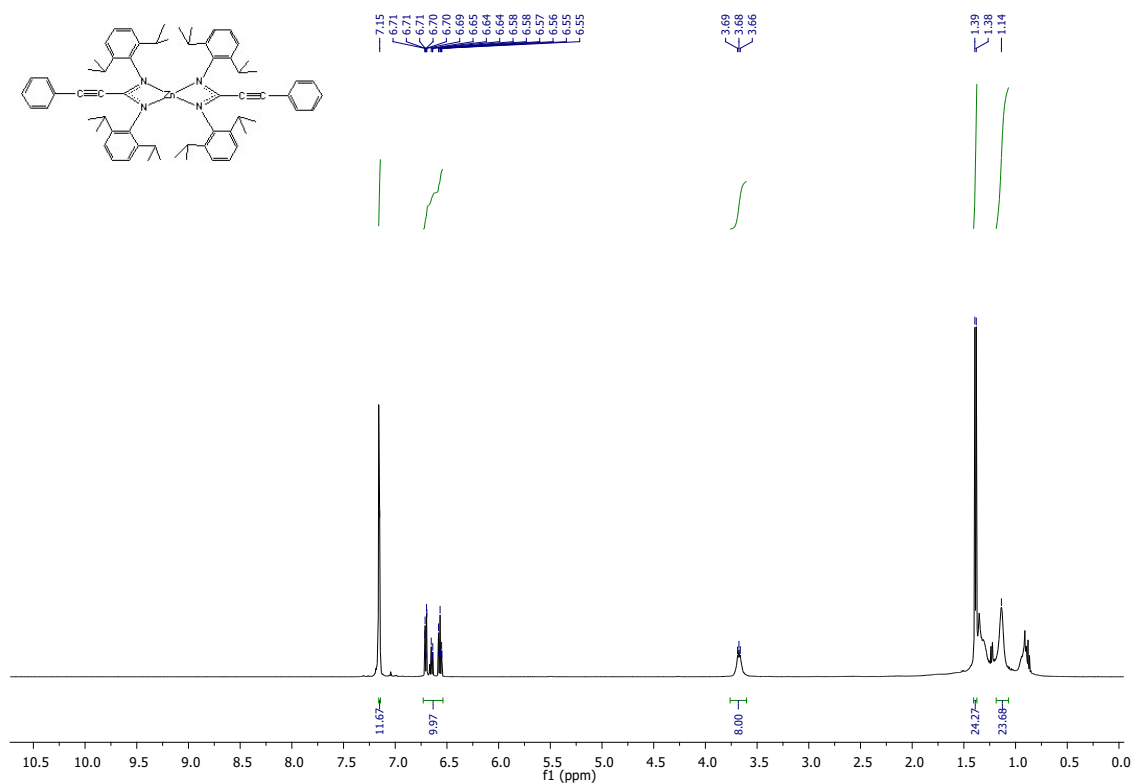


**Figure S22.** <sup>1</sup>H-NMR full chart for 6 in C<sub>6</sub>D<sub>6</sub>.

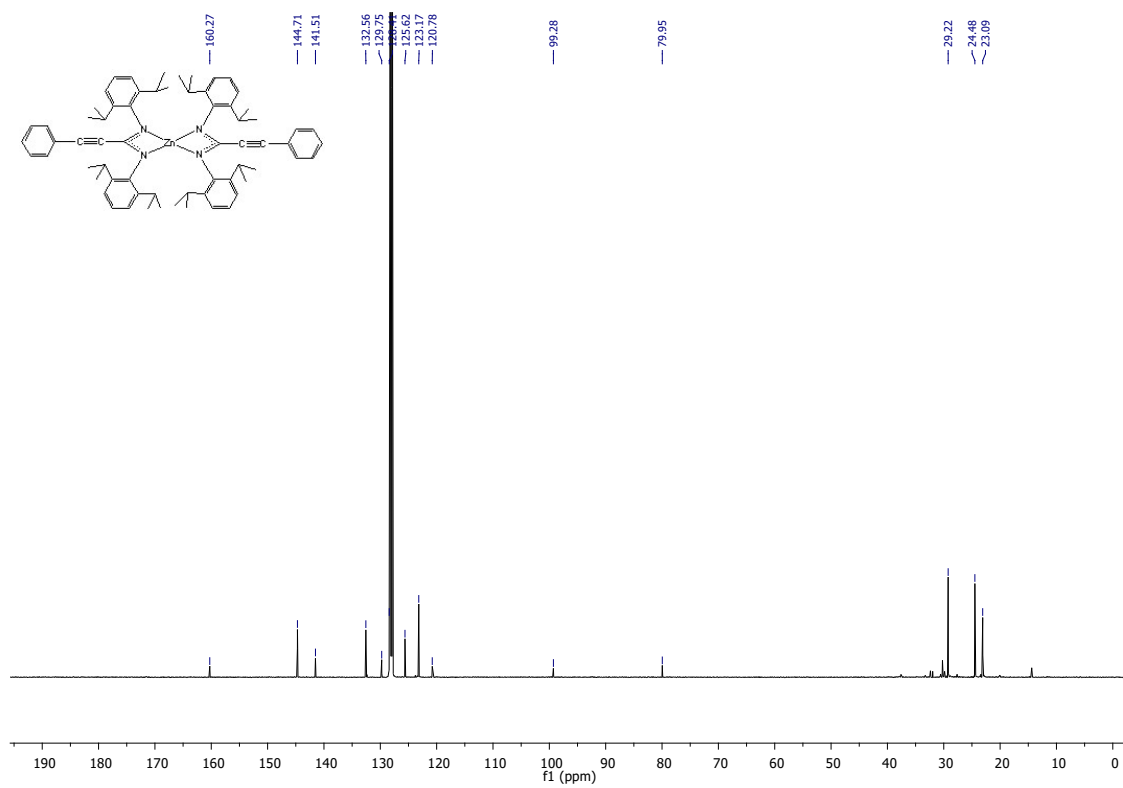


**Figure S23.** <sup>13</sup>C-NMR full chart for 6 in C<sub>6</sub>D<sub>6</sub>.

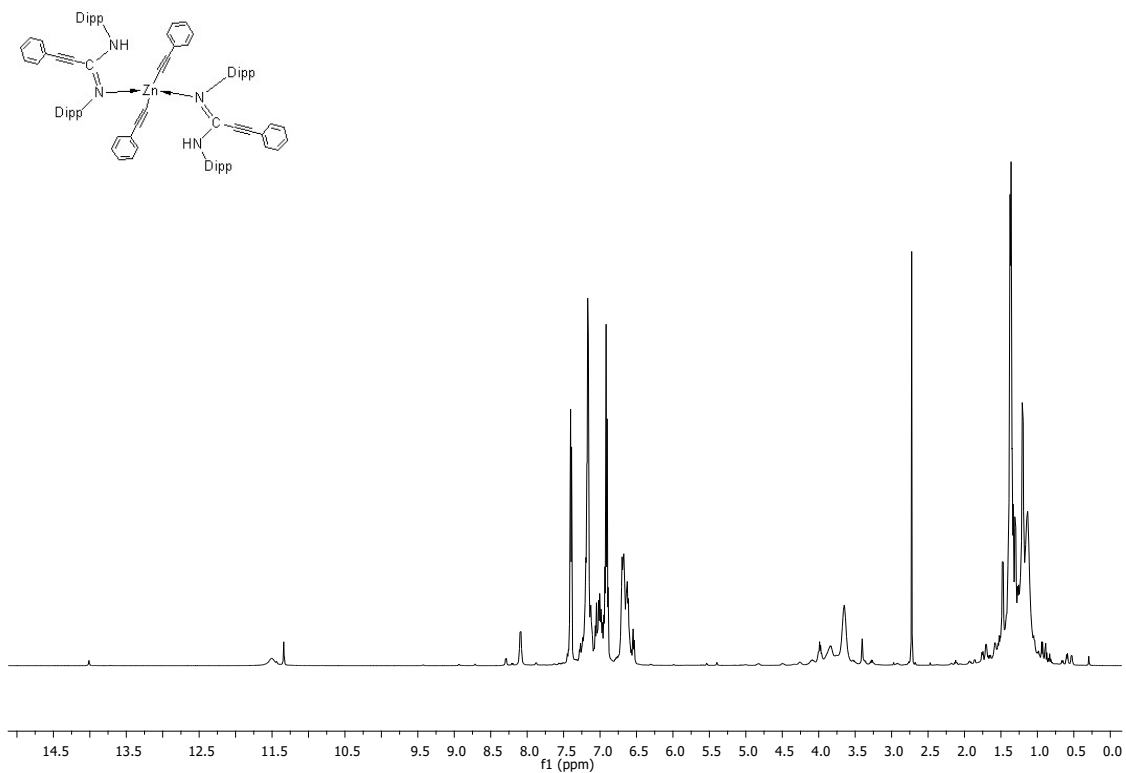


**Figure S24.**  $^1\text{H-NMR}$  full chart of reaction between bisamidinate **6** and phenylacetylene **3a** at room temperature to give rise to intermediate **7**.

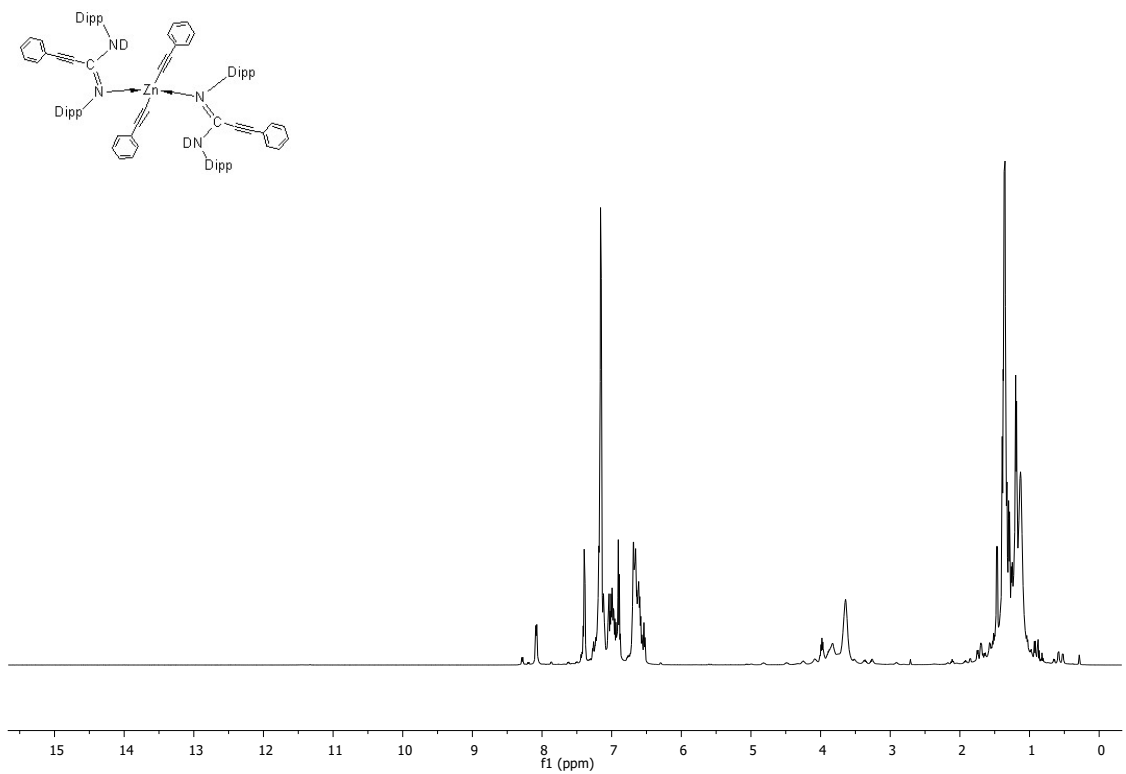


**Figure S25.**  $^1\text{H-NMR}$  full chart of reaction between bisamidinate **6** and phenylacetylene-d **3e** at room temperature.

#### 4.- X-ray structural analyses

Crystals were mounted on a glass fibre and cooled to the 100 K for compound **4a**, 250 K for compound **6** and room temperature for compounds **4b** and **4f**. Data for compounds **4a**, **4b** and **6** were collected on a Bruker APEX II CCD-based diffractometer equipped with a graphite monochromated MoK $\alpha$  radiation source ( $\lambda=0.71073$  Å). Intensities were integrated in SAINT [3] and absorption corrections based on equivalent reflections were applied using SADABS. [4] For compound **4f** data were collected on an Oxford Diffraction Xcalibur Nova single crystal diffractometer, using CuK $\alpha$  radiation. Images were collected at a 62 mm fixed crystal-detector distance using the oscillation method, with 1.0-1.2° oscillation and variable exposure time per image. Data collection strategy was calculated with the program CrysAlis Pro CCD, [5] and data reduction and cell refinement were performed with the program CrysAlis Pro RED. [5] An empirical absorption correction was applied using the SCALE3 ABSPACK algorithm as implemented in the program CrysAlis Pro RED. Structures were solved using ShelXT, [6] all of the structures were refined by full matrix least squares against  $F^2$  in ShelXL [7, 8] using Olex2. [9] All of the non-hydrogen atoms were refined anisotropically, while all of the hydrogen atoms were located geometrically and refined using a riding model. Compounds **4b**, **4f** and **6** show some disordered fragments/solvent molecule and the occupancies of the disordered group were refined with their sum set to equal 1 and subsequently fixed at the refined values. Restraints were applied to maintain sensible thermal and geometric parameters. The X-ray crystallographic coordinates for structures reported in this study have been deposited at the Cambridge Crystallographic Data Centre (CCDC) under deposition numbers 2346809-2346812 for **4a**, **4b**, **4f** and **6** respectively. These data can be obtained free of charge via [http://www.ccdc.cam.ac.uk/data\\_request/cif](http://www.ccdc.cam.ac.uk/data_request/cif)

**Table 3.** Crystal data and structure refinement for **4a**, **4b** and **4f**.

Identification code	<b>4a</b>	<b>4b</b>	<b>4f</b>	<b>6</b>
Empirical formula	C <sub>41</sub> H <sub>46</sub> N <sub>2</sub>	C <sub>49</sub> H <sub>56</sub> N <sub>2</sub> O <sub>2</sub>	C <sub>33</sub> H <sub>30</sub> N <sub>2</sub>	C <sub>264</sub> H <sub>312</sub> N <sub>16</sub> Z n <sub>4</sub>
Formula weight	566.80	704.95	454.59	3970.76
Temperature/K	250.0	296.15	298.15	250.0
Crystal system	orthorhombic	triclinic	monoclinic	orthorhombic
Space group	Pbca	P-1	P2 <sub>1</sub> /n	Pbcn

a/Å	18.7643(7)	9.426(2)	12.3909(2)	20.6268(7)
b/Å	17.8153(7)	10.912(2)	15.7998(3)	16.0836(6)
c/Å	20.5885(6)	21.672(5)	13.9004(2)	18.5709(6)
$\alpha$ /°	90	102.253(3)	90	90
$\beta$ /°	90	97.132(3)	99.625(2)	90
$\gamma$ /°	90	103.187(3)	90	90
Volume/Å <sup>3</sup>	6882.6(4)	2085.7(8)	2683.03(8)	6161.0(4)
Z	8	2	4	1
$\rho_{\text{calc}}$ /cm <sup>3</sup>	1.094	1.122	1.125	1.070
$\mu$ /mm <sup>-1</sup>	0.063	0.067	0.497	0.438
F(000)	2448.0	760.0	968.0	2128.0
Crystal size/mm <sup>3</sup>	0.25 × 0.241 × 0.153	0.3 × 0.3 × 0.25	0.485 × 0.238 × 0.163	0.245 × 0.181 × 0.176
Radiation	MoK $\alpha$ ( $\lambda$ = 0.71073)	MoK $\alpha$ ( $\lambda$ = 0.71073)	Cu K $\alpha$ ( $\lambda$ = 1.54184)	MoK $\alpha$ ( $\lambda$ = 0.71073)
2 $\theta$ range for data collection/°	6.722 to 52.906	4.822 to 50.688	8.54 to 138.996	3.212 to 50.806
Index ranges	-23 ≤ h ≤ 23, -22 ≤ k ≤ 22, -25 ≤ l ≤ 24	-11 ≤ h ≤ 11, -12 ≤ k ≤ 13, -26 ≤ l ≤ 26	-14 ≤ h ≤ 14, -16 ≤ k ≤ 19, -15 ≤ l ≤ 16	-24 ≤ h ≤ 24, -19 ≤ k ≤ 19, -17 ≤ l ≤ 22
Reflections collected	75958	14371	14574	55520
Independent reflections	7064 [ $R_{\text{int}}$ = 0.0358, $R_{\text{sigma}}$ = 0.0207]	7460 [ $R_{\text{int}}$ = 0.0353, $R_{\text{sigma}}$ = 0.0655]	4968 [ $R_{\text{int}}$ = 0.0274, $R_{\text{sigma}}$ = 0.0238]	5669 [ $R_{\text{int}}$ = 0.0519, $R_{\text{sigma}}$ = 0.0303]
Data/restraints/parameters	7064/0/396	7460/198/519	4968/66/350	5669/438/420
Goodness-of-fit on $F^2$	1.030	1.017	1.035	1.049
Final R indexes [ $I \geq 2\sigma(I)$ ]	$R_1$ = 0.0427, $wR_2$ = 0.1055	$R_1$ = 0.0588, $wR_2$ = 0.1430	$R_1$ = 0.0429, $wR_2$ = 0.1224	$R_1$ = 0.0805, $wR_2$ = 0.2314
Final R indexes [all data]	$R_1$ = 0.0646, $wR_2$ = 0.1197	$R_1$ = 0.1216, $wR_2$ = 0.1779	$R_1$ = 0.0481, $wR_2$ = 0.1293	$R_1$ = 0.1392, $wR_2$ = 0.2956
Largest diff. peak/hole / e Å <sup>-3</sup>	0.15/-0.21	0.18/-0.23	0.17/-0.16	0.48/-1.08

## 5- Computational methods

All DFT calculations were carried out using the GAUSSIAN16 package [10], and the M06L functional [11]. A pruned numerical integration grid (99,590) was used for all the calculations via keyword Int=Ultrafine, together with the empirical dispersion correction from Grimme and co-workers via keyword GD3 [12]. Effective core potentials and their associated double- $\zeta$  LANL2DZ basis set were used for Zn [13]. The light elements (C, H and N) were described using the 6-31G\* basis [14]. Geometry optimizations were performed under no symmetry restrictions, using analytical gradient techniques, and starting from initial coordinates derived from X-ray data when available. Transition States were searched for, either by using Synchronous Transit-Guided Quasi-Newton (STQN) methodologies (keywords QST2 or QST3), or by the “distinguished reaction coordination procedure” by choosing an internal coordinate (typically a distance) as reaction coordinate and running an energy scan calculation along it, with the maxima of this plot being then used as starting point for a conventional transition state optimization. Frequency analysis was performed for all the stationary points to ensure that either, a minimum structure with no imaginary frequencies, or a saddle point with only one negative frequency along the reaction coordinate, were achieved. This calculation also provides thermochemical information about the reaction pathways at 298.15 K and 1 atm using the harmonic approximation. The connectivity of the optimized transition states was fully corroborated in the forward and backward direction via IRC calculations, or by manual displacement of the geometrical parameters along the negative frequency and further optimization of the resulting geometries. Solvation effects (toluene) were modelled by using the SMD variation of IEFPCM of Truhlar and workers [15] via the SMD option in Gaussian SCRF keyword. Following previously described procedures [16], differences in translational and rotational entropy when going from ideal gas to solution were considered by the addition of an energy contribution equal to  $8RT$  (*ca.*  $4.74 \text{ kcal}\cdot\text{mol}^{-1}$ ) to the Gibbs free energy of all the species. Also, the effect of concentration (going from a reference state of 1 atm to 1M) was considered by addition of an energy contribution of  $RT\cdot\ln(P_{1M}/P_{1atm})$  (*ca.*  $1.89 \text{ kcal}\cdot\text{mol}^{-1}$ ) to all the species [15]. Figures S24 and S25 display the computed reaction profiles for all the species in terms of electronic energies and corrected Gibbs free energies, respectively.

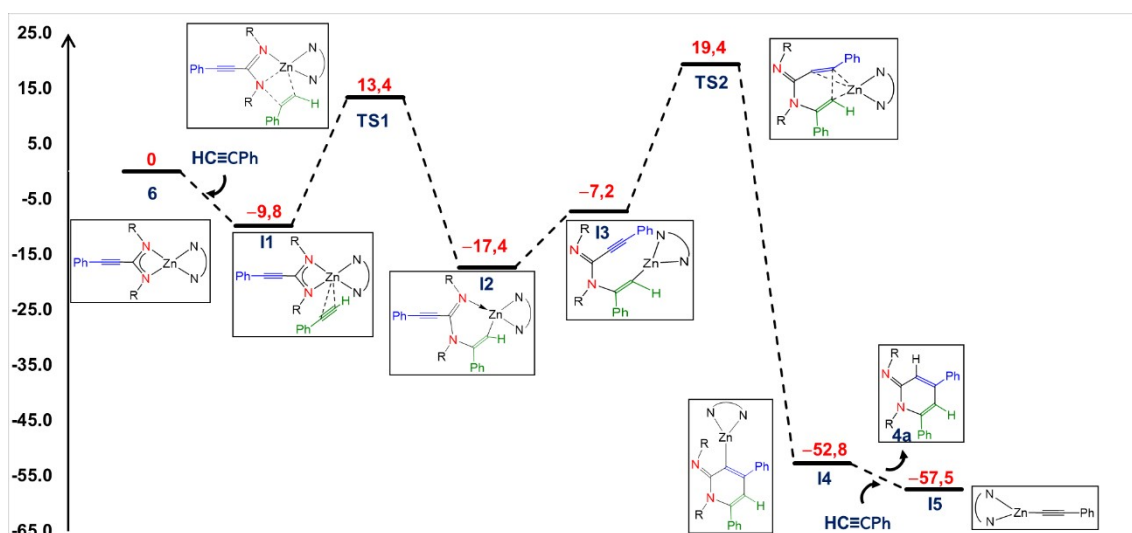


**Figure S26.** DFT-computed reaction profile for the formation of **4a** from DippNCNDipp and HCCPh catalyzed by the bis(aminidinato) complex **6** (Electronic energies expressed in kcal mol<sup>-1</sup>).

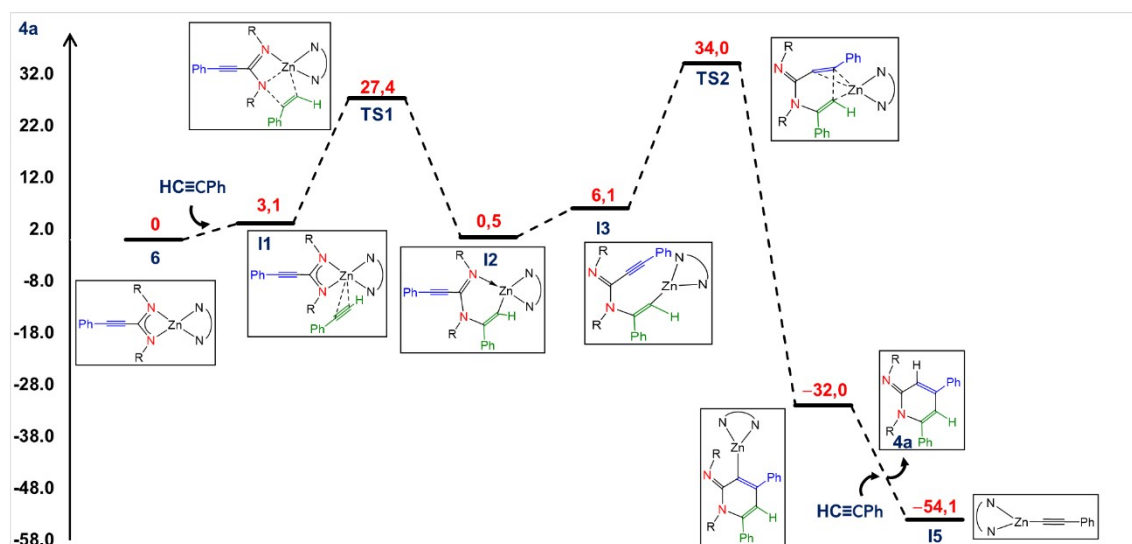


**Figure S27.** DFT-computed reaction profile in solution (toluene) for the formation of **4a** from DippNCNDipp and HCCPh catalyzed by the bis(aminidinato) complex **6** (entropy + concentration corrected Gibbs free energies expressed in kcal mol<sup>-1</sup>).

## 6.- References

- [1] A.J. Melchor Bañales, M.B. Larsen, Thermal Guanidine Metathesis for Covalent Adaptable Networks. *ACS Macro Lett.*, **2020**, 9, 937–943. DOI: 10.1021/acsmacrolett.0c00352.
- [2] A., Martínez, S., Moreno-Blázquez, A., Rodríguez-Diéguez, A., Ramos, R., Fernández-Galán, A., Antiñolo, F. Carrillo-Hermosilla, Simple ZnEt<sub>2</sub> as a catalyst in carbodiimide hydroalkynylation: structural and mechanistic studies. *Dalton Trans.*, **2017**, 46, 12923-12934. DOI: 10.1039/c7dt02700a.

- [3] Bruker, SAINT+ v8.38A Integration Engine, Data Reduction Software, Bruker Analytical X-ray Instruments Inc., Madison, WI, USA, 2015.
- [4] Bruker, SADABS 2014/5, Bruker AXS area detector scaling and absorption correction, Bruker Analytical X-ray Instruments Inc., Madison, Wisconsin, USA, 2014/5.
- [5] CrysAlis Pro; Oxford Diffraction Limited, Ltd.: Oxford, U. K., 2006.
- [6] G.M. Sheldrick, *Acta Crystallogr. Sect. A: Found. Crystallogr.* **2015**, 71, 3-8.
- [7] G.M. Sheldrick, *Acta Crystallogr. Sect. A: Found. Crystallogr.* **2008**, 64, 112-122.
- [8] G.M. Sheldrick, *Acta Crystallogr. Sect. C: Struct. Chem.* **2015**, 71, 3-8.
- [9] O.V. Dolomanov, L. J. Bourhis, R. J. Gildea, J. A. K. Howard, H. J. Puschmann, *Appl. Crystallogr.* **2009**, 42, 339-341
- [10] M.J. Frisch, G.W. Trucks, H.B. Schlegel, G.E. Scuseria, M.A. Robb, J.R. Cheeseman, G. Scalmani, V. Barone, G.A. Petersson, H. Nakatsuji, X. Li, M. Caricato, A.V. Marenich, J. Bloino, B.G. Janesko, R. Gomperts, B. Mennucci, H.P. Hratchian, J.V. Ortiz, A.F. Izmaylov, J.L. Sonnenberg, D. Williams-Young, F. Ding, F. Lipparini, F. Egidi, J. Goings, B. Peng, A. Petrone, T. Henderson, D. Ranasinghe, V.G. Zakrzewski, J. Gao, Rega, N.; G. Zheng, W. Liang, M. Hada, M. Ehara, K. Toyota, R. Fukuda, J. Hasegawa, M. Ishida, T. Nakajima, Y. Honda, O. Kitao, H. Nakai, T. Vreven, K. Throssell, J.A. Montgomery, Jr., J.E. Peralta, F. Ogliaro, M.J. Bearpark, J.J. Heyd, E.N. Brothers, K.N. Kudin, V.N. Staroverov, T.A. Keith, R. Kobayashi, J. Normand, K. Raghavachari, A.P. Rendell, J.C. Burant, S.S. Iyengar, J. Tomasi, M. Cossi, J.M. Millam, M. Klene, C. Adamo, R. Cammi, J.W. Ochterski, R.L. Martin, K. Morokuma, O. Farkas, J.B. Foresman, D.J. Fox, Gaussian 16, Revision A.03, Gaussian, Inc., Wallingford CT, USA, 2016.
- [11] Y. Zhao, D.G. Truhlar, *J. Chem. Phys.*, **2006**, 125, 194101.
- [12] S. Grimme, J. Antony, S. Ehrlich, H. Krieg, *J. Chem. Phys.*, **2010**, 132, 154104.
- [13] P.J. Hay, W.R. Wadt, *J. Chem. Phys.*, **1985**, 82, 299.
- [14] P.C. Hariharan, J.A. Pople, *Theor. Chim. Acta*, **1973**, 28, 213. b) G.A. Petersson, M.A. AlLaham, *J. Chem. Phys.*, **1991**, 94, 6081. (c) G.A. Petersson, A. Bennett, T.G. Tensfeldt, M.A. Al-Laham, W.A. Shirley, J.A. Mantzaris, *J. Chem. Phys.*, **1988**, 89, 2193.
- [15] A.V. Marenich, C.J. Cramer, D.G. Truhlar, *J. Phys. Chem. B*, **2009**, 113, 6378.
- [16] a) Y.B. Yu, P.L. Privalov, R.S. Hodges, *Biophys. J.*, **2001**, 81, 1632. b) E. Wilhelm, R. Battino, *Chem. Rev.*, **1973**, 73, 1. c) L. Falivene, V. Barone, G. Talarico, *Mol. Catal.*, **2018**, 452, 138. d) J. Chen, A. Motta, J. Zhang, Y. Gao, T.J. Marks, *ACS Catal.* **2019**, 9, 8810.